TABLE OF CONTENTS

NASA Contractor Report 3204

Determination of Physical and Chemical States of Lubricants in Concentrated Contacts - Part 1

James L. Lauer

GRANT NSG-3170
NOVEMBER 1979

NASA

NASA Contractor Report 3204

Determination of Physical and Chemical States of Lubricants in Concentrated Contacts - Part 1

James L. Lauer
Rensselaer Polytechnic Institute
Troy, New York

Prepared for
Lewis Research Center
under Grant NSG-3170

National Aeronautics
and Space Administration

**Scientific and Technical
Information Branch**

1979

Blank Page

TABLE OF CONTENTS

1. INTRODUCTION

The work reported here for 1978 was a continuation of our previous effort at Suntech, Inc. under contract NAS3-19758[1]. In a corporate decision by Sun Oil Company, the owners of Suntech, Inc., the project had to be discontinued there, but much of the apparatus was transferred to me for the new laboratory at Rensselaer Polytechnic Institute (R.P.I.). The Department of Mechanical Engineering, Aeronautical Engineering and Mechanics of R.P.I. provided not only facilities, but some very important new equipment to allow me to continue the work under NASA Grant NSG 3170.

While these changes will, without question, benefit this work--and have already--a very substantial portion of the 1978 effort had to be devoted to the setting up of the new laboratory. Equipment contained in some 200 boxes had to be installed. New coworkers had to be instructed (my long-time associate, Mr. M.E. Peterkin, was assigned to non-research work at Sun Oil Company). I had to become adjusted to the new environment.

The principal new additions to our instrumentation are a vibration-resistant table and a dedicated minicomputer. As so often is the case, a change of one part requires a change of another and so the table required a superior method of mounting the motor driving our mockup bearing--in order to make use of the improvement provided by the table. Similarly, the minicomputer required changes in the computer programs for processing the data and completely new interfaces.

Every possible effort was made to make the system--our infrared emission microinterferometer for obtaining spectra from a sliding elastohydynamic (ehd) bearing contact,our high-pressure calibration apparatus using diamond anvil cells, the ruby fluorescence pressure gauge, the Perkin-Elmer attenuated total reflectance spectrometer and other essential apparatus--operational and to

collect a reasonable amount of data before the end of 1978. This goal was achieved and a number of ehd contact emission spectra and attenuated total reflection spectra were obtained. The presence of polarization and thus alignment of lubricant molecules was confirmed. Temperature gradients through ehd films were definitely observed. A beginning was made toward their analytical treatment. This work formed the basis of a number of presentations and publications.

As in the past, the Air Force Office of Scientific Research co-sponsored the more fundamental aspects of this work under Grant No. AFOSR-78-3473. The cooperation between the two agencies made our work more efficient and thus more productive for both.

2. THEORY OF GENERATION, IN EHD CONTACTS, OF INFRARED EMISSION SPECTRA

Because reproducibility of our spectra from operating contacts is now better than was previously achieved, the evidence of a temperature gradient within an ehd lubricating film is now sufficiently convincing to make a detailed mathematical analysis worthwhile. A beginning in this direction was made by us some time ago[1]; the present analysis brings it closer to the goal of determining the gradient. It could be very important to ehd lubrication, since it could point toward partial glass formation, for example.

In contrast to the usual conditions of infrared emission spectroscopy where a thin layer of an organic material is radiating from a highly reflecting support and the temperature of both layer and support are assumed to be equal, the conditions of an ehd film in an operating contact involve non-uniform temperature and pressure and a non-uniform flow velocity. Heat is generated in the lubricant by viscous friction while the solid boundaries are heat sinks. Convection removes most of the heat. However, the following analysis considers only radiation heat transfer under local radiation equilibrium and is a pragmatic approach for the interpretation of infrared emission spectra. The method was adopted from Viskanta and coworkers[2] and is based on the radiation transfer equation (RTE) developed by the astrophysicists[3]. It provides a gereral framework, applicable to a variety of situations, while the more common ray tracing procedures must be developed separately for every case.

Fig. 1 illustrates the basic model. It can be extended to more realistic situations quite readily. A film of thickness L is covering an opaque material, such as a metal surface. The film is "semi-transparent", i.e. transparent at most infrared frequencies, but absorbing at selected ones. An example of such a film is oil spread on a polished metal plate. The film/metal interface is

assumed to be smooth, but the model is readily changed to take a rough surface into account. The model is one-dimensional or cylindrically (azimuthally) symmetrical about the optic axis of the objective lens collecting the radiation.

The RTE to be solved for such a slab bounded by two parallel surfaces is

$$\cos\theta \cdot \frac{dI_\nu(y,\cos\theta)}{dy} = -\kappa_\nu(y)\left[n_\nu^2(y)\, I_{b\nu}(y) - I_\nu(y,\cos\theta)\right] \qquad (1)$$

Azimuthal symmetry is assumed; $I_\nu(y,\theta)$ is the monochromatic intensity (radiance) at frequency ν and in a direction forming an angle θ with y, the distance from the exit surface of the slab; $\kappa_\nu(y)$ is the spectral absorption coefficient, $n_\nu(y)$ is the index of refraction in the film and $I_{b\nu}(y)$ is the radiance given by the Planck blackbody function corresponding to the temperature $T(y)$, which is assumed to vary with y in a continuous manner.

Equation 1 might not be familiar to many spectroscopists. Its derivation is given in many places[2,3]; it merely states that the change in radiance with distance is the difference between the radiation emitted (first term on the right) and the radiation absorbed (second term on the right).

It has become customary to separate I into an outgoing component $I^+(\cos\theta>0)$ and an ingoing component $I^-(\cos\theta<0)$. The boundary conditions for (1) then become

$$I_\nu^-(0,\cos\theta) = \rho_{1\nu}\, I_\nu^+(0,\cos\theta)\ ;\ \cos\theta<0 \qquad (2)$$

and

$$I_\nu^+(L,\cos\theta) = \varepsilon_{2\nu}(\cos\theta)\, n_\nu^2 I_{b\nu}(L) + \rho_{2\nu}(\cos\theta) I_\nu^-(L,\cos\theta) \qquad (3)$$

$$I_\nu(L) \equiv I_\nu(M)$$

where $\rho_\nu(\cos\theta)$ is the spectral directional reflectivity of the interface and $\varepsilon_{2\nu}(\cos\theta)=1-\rho_{2\nu}(\cos\theta)$, is the spectral emittance. Equation (1) is easily solved by an integrating factor and since Snell's law gives

$$n_\nu \sin\theta = n_{o\nu} \sin\theta' \qquad (4)$$

the solution of Eq. (1) for the spectral intensity emerging outwardly from the layer can be written as

$$I_\nu^+(0,\cos\theta') = [1-\rho_{1\nu}(\cos\theta)]\cdot(n_{o\nu}/n_\nu)^2/\beta_\nu(\tau_{L\nu},\cos\theta)\cdot$$
$$\cdot\left\{[1-\rho_{2\nu}(\cos\theta)]n_\nu^2 I_{b\nu}(M)\cdot e^{-\tau_{L\nu}/\cos\theta} + \right.$$
$$\left. + \int_0^L n_\nu^2 I_{b\nu}(y)\cdot\left[e^{-\tau_\nu/\cos\theta} + \rho_{2\nu}(\cos\theta)\, e^{-(2\tau_{L\nu}-\tau_\nu)/\cos\theta}\right]\right\}\cdot$$
$$\cdot\kappa_\nu\, dy/\cos\theta \qquad \text{for } \cos\theta>0 \qquad (5)$$

$$\text{where } \beta_\nu(\tau,\cos\theta) \equiv \left[1-\rho_{1\nu}(\cos\theta)\rho_{2\nu}(\cos\theta)e^{-2\tau_{L\nu}/|\cos\theta|}\right]^{-1} \qquad (6)$$

is the factor accounting for multiple reflections between interfaces 1 and 2, $I_{b\nu}(M)$ is the blackbody radiance corresponding to the metal surface, and the optical depth τ_ν and thickness $\tau_{L\nu}$ are defined, respectively, as

$$\tau_\nu = \int_0^y \kappa_\nu(y)\, dy \qquad (7)$$

$$\text{and} \qquad \tau_{L\nu} = \int_0^L \kappa_\nu(y)\, dy \qquad (8)$$

The radiant flux of wave number $\tilde{\nu}$ entering the instrumentation is the spectral intensity integrated over the solid angle of the objective. The first term in

the curly brackets of Eq. (5) is the radiance of the metal surface attenuated by passage through the film and partial reflectance at the boundaries. It could have been derived simply by inspection and application of Beer's law of absorption. The second term, the integral, takes into account the emission of radiation by the film itself.

An advantage of the above formalism is the ease with which the spatial dependence of absorption coefficient, index of refraction, and spectral radiance can be taken into account. Extension from one dimension to three dimensions is also quite straightforward.

With the definition of $k = \kappa/\cos\theta$, the dropping of the monochromatic frequency subscript and the angular dependence subscript of the reflectivity and the radiance, the above equation can be rewritten as

$$I^{+}(0, \cos\theta') = (1-\rho_2)(n_0/n)^2 \beta \left\{(1-\rho_1) n^2 I_b(M) e^{-kL} + \right.$$
$$\left. + \int_0^L n^2 I(y) \left[e^{-ky} + \rho_2 e^{-k(2L-y)}\right] \right\} k\, dy \qquad (9)$$

since $\tau = ky$ and $\tau_L = kL$.

This is the basic equation which will now be solved for some of our experimental situations. It will be noted that the temperature distribution through the layer $T(y)$ can be determined, in principle, from measurements of I^{+} and solving for $I(y)$, $I_b(M)$ being known, $k(y)$ and $n(y)$ being assumed known or preferably, constant with respect to temperature. Eq. (9) then becomes a non-linear Fredholm integral equation of the first kind for the unknown function $I(y)$ for which a number of methods of solutions are possible. Viskanta and co-workers [2] used such a procedure to determine the temperature in slabs of cooling glass.

A few solutions of Eq. (9) pertaining to this work will now be discussed.

(i) Uniformly Heated Film between Identical Interfaces

An example of this situation is a semi-transparent fluid (or solid) in a high-pressure diamond cell.

In this case, n, k, $\rho_1=\rho_2=\rho$ and $I_{(\nu)}$ are constants, and the source term, $I_b(M)$ can be set equal to zero since no external heat sources are considered. The solution of Eq. 9 is then

$$I^+ = \frac{(1-\rho)(1-e^{-kL})}{1-\rho e^{-kL}} I_b(T) \qquad (10)$$

where T is the uniform temperature of the slab. Since we can define an effective emissivity ε_1 as the ratio I^+/I_b and $t=e^{-kL}$ as the transmissivity, we can write (10) in the form

$$\varepsilon_1 = \frac{(1-\rho)(1-t)}{1-\rho t} \qquad (11)$$

which is McMahon's relation. It shows very clearly that a non-absorbing material cannot emit radiation, for $\varepsilon=0$ when $t=1$.

(ii) Film on a metal surface, both at the same temperature.

This is the usual situation for obtaining emission spectra, e.g. Griffith[4] obtained emission spectra of thin layers of grease in this way, but noted that thicker layers did not give good spectra, presumably--we believe--because these layers could not be maintained at uniform temperatures.

By setting $I(M) = I(g) = I$ Equation (9)

yields

$$I^{+} = (1-\rho_1)\beta I \left[(1-\rho_2)e^{-kL} - e^{-kL} + 1 + \rho_2 (e^{-kL} - e^{-2kL})\right]$$

from which an effective emissivity of

$$\varepsilon_2 = \frac{(1-\rho_1)(1-\rho_2 t^2)}{1-\rho_1\rho_2 t^2} \qquad (12)$$

can be derived.

The dependence of the effective emissivity on the square of the transmissivity should not be surprising since the metallic mirror backing effectively doubles the film thickness. The pairing of reflectivity ρ_2 with the film transmissivity t indicates the importance of a high reflectivity--unity, if possible--for maximum sensitivity of the spectrum to the film transmissivity. Under these conditions, the metal does not contribute to the spectrum at all.

If the film merely attenuated and reflected the radiation emanating from the metal surface, the emissivity--corresponding to the first term of Eq. (11) or from first principles--would be

$$\varepsilon_3 = \frac{(1-\rho_1)(1-\rho_2 t^2)}{1-\rho_1\rho_2 t^2} \qquad (13)$$

The difference between ε_2 and ε_3 is the contribution of the film, viz.

$$\varepsilon_4 = \varepsilon_2 - \varepsilon_3 = \frac{\rho_2 t(1-t)}{1-\rho_2\rho_1 t} \qquad (14)$$

Clearly, ε_4 is maximized when $t=\frac{1}{2}$, which establishes a criterion for the optimum film thickness-under conditions of temperature uniformity.

(iii) Film on a metal surface; uniform temperature different from metal surface temperature.

Equation (9) now becomes

$$I^+ = (1-\rho_2)\beta n_0^2\left[(1-\rho_1)t\, I_b(M) + I_b(T_1)\cdot(1-t)(1+\rho_2 t)\right] \qquad (15)$$

This is an approximation to the situation in a bearing; the lubricant temperature may be different from the metal surface temperature and, in fact, there is usually a temperature gradient through the lubricant film itself. It is now difficult to define an emissivity for the general case, since two sources of radiation are at different temperatures.

It is easy to see that for equal metal and film temperatures Eq. (15) reduces to Eq. (14) as expected. For the metal temperature much lower than the film temperature, $I_b(M) \ll I_b(T_1)$ and an effective emissivity

$$\varepsilon_6 = \frac{(1-\rho_2)(1-t)(1+\rho_2 t)}{1-\rho_1\rho_2 t^2} \qquad (16)$$

can be evaluated. Comparison of Eq. (16) with Eq. (13) shows that the cold

metal produces an enhanced emissivity of the film for the same temperature, because the third factor in the numerator, a term containing the metal surface reflectivity, will, in general, exceed unity. It will be equal to unity for $t=0$, i.e. a completely opaque film, say at the frequency of an absorption peak. In this case Eq. (15) shows that the radiant intensity will then always be independent of the radiance of the metal, i.e. of the metal temperature, and the effective emissivity,

$$\varepsilon_1 = I^+ / n_0^2 I_b(T_1) = 1 - \rho_1 \qquad (17)$$

is entirely independent of anything behind the front radiating surface; i.e. the film forms an effective "dam" for the situation behind it.

Let us now suppose that the metal surface is hotter than the uniform film temperature and the emitted radiation is observed at a frequency significantly higher or lower than that of the lubricant's absorption peak. This situation could occur, for example, when direct metal-to-metal contact takes place at asperities. Now the emissivity at the observed frequency, ε_β, as calculated from Eq. (15), will reduce to that of Eq. (13), or

$$\varepsilon_\beta = \frac{I^+}{n_0^2 I_b(M)} = \frac{(1-\rho_1)(1-\rho_2)t}{1-\rho_1\rho_2 t} \qquad (18)$$

The total radiant power is now proportional to the blackbody radiance at the metal temperature and not at the film temperature. Since the former has been postulated to be higher than the latter

$$\varepsilon_1 I_b(T_1) > \varepsilon_\beta I_b(M) \qquad (19)$$

the radiance at the peak of an infrared band, where the transmittance of the fluid is zero, will be less than the radiance at nearby frequencies. A plot of radiance versus frequency will, for this situation, show an apparent absorption band.

Is it possible to have an emission band, possibly with a dimple at the peak (peak inversion), solely by having the metal boundary hotter than the lubricant film temperature in any infrared spectral region? Evidently not, as long as ρ_2 (Eq.15) is frequency-independent, since we would be requiring I^+ to be a maximum at a frequency other than that where t=0. The reflectivity, and hence the emissivity, of a metal surface is unlikely to show a strong frequency dependence centered about an absorption peak of the lubricant.

On the other hand, it is possible to have emission bands with self-absorbed peaks, when the radiation emitted by a layer of lubricant traverses a cooler layer of the same lubricant before reaching the detector. The reason is that the width of condensed phase emission (or absorption) bands increase with temperature (Rakov[5]) while the intensities decrease somewhat. Since emission and absorption bandwidths are essentially equal for equal temperatures, self-absorption by a cooler layer will appear as a dimple on a wide peak.

For example, a Gaussian emission band of the form

$$f(\nu) = \text{const} \cdot e^{-\frac{1}{2}\left(\frac{\nu-a}{\sigma}\right)^2} \qquad (20)$$

is characterized by the peak frequency and the full-width at half-maximum, which is generally called the half-width Γ. From the above definition

$$\Gamma = 2.354\sigma \qquad (21)$$

Thermal movement of molecules in liquids (Brownian movement) consist of irregular oscillations or rotations about a temporary unstable state of equilibrium. According to Frenkel's theory of the liquid state and Eyring's theory of viscosity, this movement proceeds in jerks, whose frequency is determined by a barrier potential, U. At least part of the band width is due to this motion (rotational or vibrational diffusions), so that

$$\Gamma \propto \frac{1}{\eta} = \text{const.} e^{-\frac{U}{kT}} \qquad (22)$$

where η is the "viscosity".* Therefore, the higher the temperature, the smaller the exponent in Eq. (22), the smaller the viscosity and the greater the bandwidth. A wide emission band may thus be superimposed by a narrow absorption band giving rise to the "dimpled" band of Fig. 2. It is characteristic of a temperature gradient within the same fluid.

The simultaneous occurrence of emission and absorption should be considered when determining temperatures of lubricants from the strengths of infrared emission.

These ideas will be expanded when more experimental data become available. However, the deduction of the existence of a temperature gradient from "dimples" seems inescapable.

---

*Several "viscosities" are defined, e.g. shear or dilation. There is considerable divergence of opinion as to which is primarily responsible for bandwidth.

2.1 Significance of Heat Generation

One of the primary functions of a lubricant is the reduction of heat generated between rubbing surfaces. Nearly all the energy dissipated by friction appears as heat; the mechanical equivalent of heat has been derived from these observations. The lubricant separates the rubbing surfaces and removes heat.

Viscous shear resistance leads to the generation of heat within the lubricant in full-fluid lubrication. Under ehd conditions heat is generated as a result of solid flexing as well and possibly even as a result of asperities interaction. Our theoretical analysis shows that dimples in infrared emission bands are definite indication of non-uniform heat generated in the fluid itself, while apparent absorption bands showing up in infrared emission spectroscopy would be caused by asperities interaction. Certainly asperities interaction is likely to produce wear and should be avoided. High temperatures in the fluid contact region would have the effect of reducing fluid viscosity and thus film thickness and the load carrying capacity of a bearing. But high temperature in the contact fluid at given film thicknesses can also be an indication of much viscous friction, making an analysis of the material influence of the physical parameters a difficult task.

The importance of heat generation to our work lies in the need for an understanding of the emission spectra (occurrence of dimples, plateaus, etc.) and of the nature and origin of traction. Since our traction fluids are generally running hotter than others and show a temperature gradient, they are likely to exhibit a unique combination of flow properties and viscosity index. Molecular alignment would be a manifestation. We believe to be on the verge of identifying such a combination of properties and of the chemical constitution responsible for it.

3. APPARATUS

3.1 Infrared Emission Interferometer

The apparatus is essentially the same as the one described previously[1]. The thermal radiation emitted from the contact region of a bearing (ball sliding over a diamond window) is collected by an all-reflecting microscope objective (Beck lens) and passed into an interferometer-spectrometer for analysis (Fig. 3). There are two parts to this radiation: (a) discrete emission bands from the lubricant and (b) continuous graybody radiation from the solid surfaces. The latter can exceed the discrete radiation from the lubricating film by orders of magnitude in overall intensity. If the total radiation were detected and analyzed simultaneously, the discrete radiation would be lost in the noise level. Discrete emission bands appear at the absorption frequencies for, in a simple-minded model, the ball's emittance is higher at these than at other frequencies, the model being that of a surface painted black in selected spectral regions. Hence, it is necessary to oppose the continuous radiation by a blackbody source. In our earlier work this was done by a chopper and reference source above the lens. However, that method proved to be impractical because (a) of the difficulty of changing lenses and (b) of the limited thermal capacity of the reference source. The present chopper and reference source are located below the lens and downstream from the 45^{o} degree mirror which changes the direction of the incoming radiation from vertical to horizontal in the interferometer's plane of incidence. Fig. 4 shows the new setup. The disadvantages of the new setup are the need for cooling the shield of the blackbody reference source to prevent the shield from radiating and the need for maintaining the lens at constant temperature since the lens, now located ahead of the chopper,

can also become an effective source. Both of these difficulties were overcome, the former by jets of nitrogen directed at the shield and the latter by placing a double plastic "tent" cover over the entire optical table. The latter problem turned out to be a major one, since the laboratory is ventilated by a heat pump system, which is subject to rather large ($\pm 5^{\circ}C$) temperature swings.

The dedicated minicomputer, which is now a part of our Michelson interferometer, is a considerable advance over the time-sharing data processing previously used. It is entirely under our control, the paper punch could be eliminated, and data can now be stored indefinitely on floppy discs. The turnaround time of the data processor is no longer the rate-determining step in our gathering of spectra: now it is the detector and the potential certainly exists to improve it. However, there was a price to be paid: the cost and time spent with interfacing, both hardware and software. The minicomputer (kindly provided for us by the Department) is a Texas Instruments Model 990/4 System. It has a FORTRAN compiler and, with the overlay operating system, just enough memory capacity to handle our work. In particular, the following work was necessary:

(i) Hardware. A multiwire line had to be laid from the digital voltmeter to the CPU with an appropriate switch to avoid respective storage of the same data point. Connections to a microprocessor (SLING) capable of converting an analog X/Y recorder to a digital recorder and providing hard-wired programs for the lettering of the output spectra had to be made.

(ii) Software. The following new programs had to be written (our main Fourier program could be adapted directly to the new processor, with only minor changes): (a) Conversion from BCD (digital voltmeter) to binary, (b) Disc storage program, (c) Changes of Fourier program subroutines for overlay operation,

(d) Program for spectra plotter. Many of these steps encountered difficulties, which had to be resolved with the help of experts from Texas Instruments.

3.2 Optical Table and Motor for EHD Measurements

The interferometer and the mockup ehd assembly on which the bearing ball is rotated are now mounted on an optical table consisting of a slab of granite, weighing more than a ton, supported on a pedestal of four air pistons. Vibrations of the floor and building are thereby minimized. However, vibrations from the motor driving the ball could still be transferred to the ehd contact region through the connecting shaft. Indeed, the vibration problem appeared to be very much aggravated over the previous state of affairs. Originally the motor was mounted on a separate table straddling the optical table.

This problem was solved by a flexible shaft connecting the motor to the ball and a means for clamping this shaft at a suitable distance from the ball so as to remove undesirable frequencies. In other words, the shaft is being "tuned" in the same manner as the string of a cello by the celloist's finger. The procedure works very well; it may require "retuning" with change of motor speed.

The table supporting the electric motor turned out to be a problem at first. It would sag and thereby upset the shaft alignment. (At Suntech the motor was supported almost directly by a steel support beam of the building.) Re-inforcement of the table by heavy steel plates solved this problem, once it was recognized. The new table was strong enough to support the 1-hp motor, which had to be purchased to replace the old 1/4-hp motor after one of the traction fluids helped burn it out.

3.3 Diamond Cells. Fluorescence Spectrometer. Infrared Grating Spectrophotometer

These instruments, useful for calibration of our spectra from operating ehd contacts, have been described in our earlier reports. Considerable amounts of time had to be expended to set them up again.

Two attachments to the Perkin-Elmer grating spectrophotometer should be mentioned. One is the beam condenser enabling us to obtain spectra from the high-pressure diamond cell and the other allows for the determination of infrared spectra of surfaces by attenuated total reflection (ATR). The latter instrumentation was used to characterize gamma-irradiated ultrahigh molecular weight polyethylene wear specimens (a small special project). This "Harrick Reflection Attachment" was updated by the addition of a "Variable Angle Attachment", consisting of a germanium hemicylinder and coupled mirrors allowing for precise measurements of angles of incidence and reflection in ATR. Although only one reflection is possible with this addition, in contrast to 5-to-10 by the normal ATR-plate, the ability of varying the incidence angle on the test surface can do more than make up for this. Furthermore, it is now possible for us to measure in the infrared, both the real and imaginary part (n and k) of a complex index of refraction of a surface, especially a metal surface, using polarized and non-polarized infrared, and thus to find changes associated with scuffing, wear and fatigue. We expect to make significant use of this new device in 1979.

3.4 Emission Spectra

The procedure developed for obtaining emission spectra from ehd contacts--still using the Golay detector, which has a slow response time but very high sensitivity--is the following: First, the apparatus is stabilized, i.e. the reference temperature is adjusted to obtain essentially no <u>average</u> (d.c.)

reading for a particular set of conditions. The purpose of this rather time-consuming procedure is the maximizing of the signal from the lubricating film. The data are recorded on a disc in the form of a scan of Michelson mirror motion against detector signal, which takes about one-half to three-quarters of an hour. (This time could be considerably--as much as 200-fold--reduced with our new Hg-Cd-Te detector, for which we already built new amplifiers, etc. However, the installation of this detector could take several months and, for this reason, had to be postponed.) The 1000 or so 16-bit BCD points collected are converted to binary numbers and convoluted by a numerical filter to obtain an interferogram for the desired frequency range. Fig. 5 shows a typical interferogram before filtering and Fig. 6 after filtering, which reduced the original 1000 points to 110 points. The Fourier transformation then yields a rather noisy spectrum, e.g. Fig. 7, which is then smoothed by the Savitzky-Golay method (Fig. 8). The spectra so obtained are very reproducible and have a resolution of about 2.5 cm^{-1}.

An aspect of the Fourier emission interferometer is the need for making separate runs for different spectral regions. Optical filters with limited passbands must be inserted for various regions of the infrared spectrum to reduce the dynamic range. Our present Ge-on-salt beamsplitter covers the 2-15 μm region, but a Mylar beamsplitter must be inserted for the far infrared. The reasons for these multiple experiments lie in the very nature of emission spectroscopy. Since most of our work with bearings involves source temperatures, which are near ambient, the peak of the Planck radiation curve is near 1000 cm^{-1} and the emitted radiant powers at both lower and higher (especially higher) frequencies are quite low. In principle, the reference would compensate for this, being equally low, but a balance of very low signals can be quite unstable. Figs. 9a, 9b, and 9c, covering the entire infrared

region for an ehd emission spectrum of 5P4E at an average temperature of 40°C, therefore represents an achievement. Comparison of these figures with the grating absorption spectrum of Fig. 10 shows the equivalence of our emission spectra to the absorption spectra--except for changes caused by the operating conditions of the bearing.

4. RESULTS

4.1 Ehd Emission Spectra of 5P4E Polyphenyl Ether

We started our work at R.P.I. with this fluid for several reasons: (i) We had obtained emission spectra of this fluid from ehd bearing contacts previously, but over a much narrower wavelength region than now possible. It seemed to make sense to try to duplicate this work under our present conditions and to expand the wavelength region. (ii) This fluid has very strong and sharp infrared bands.

Figures 11 and 12 show a series of spectra. In the top row (Fig. 11) (a) the non-polarized spectrum,(b) the spectrum polarized in the conjunction plane, and (c) the spectrum polarized in a plane perpendicular to the conjunction plane are shown. The fluid reservoir temperature was essentially ambient, the average pressure in the contact was 500 MPa and the linear sliding speed of the ball over the diamond window 0.7 m/sec. The corresponding spectra in the bottom row are for the same conditions except that the speed was doubled. The spectral range of 630 to 1230 cm^{-1} is double of what was possible for us earlier so that more essential features can be shown.

Let us look at the unpolarized spectra of Fig. 11a first. No major spectral changes occurred as the speed was increased. The spectra are very similar to the standard emission or absorption spectra of 5P4E (Fig. 10a) except for relative peak intensities. Other authors[6] have observed similar differences and given various general reasons for them, (e.g. the intensity of a fundamental absorption line increases with decrease of temperature, but of an emission line with increase of temperature; absorption line intensities depend on the first power of the wavenumber, but emission line intensities on the fourth power) but detailed analyses for liquids are still lacking. The

most interesting spectral change with speed in Fig. 11a is the appearance of the 750/780 cm^{-1} structure, which is a doublet at low speed and a single band with shoulders on each side at high speed. The standard absorption spectrum of Fig. 10b shows this structure as a doublet which, moreover, is more intense than either of its neighbors, while it is much weaker in the contact emission spectra.

Why the change? We repeated some of these runs and found the same behavior all the time. Our experimental reproducibility, thanks largely to the new vibration-resistant optical table, is now very much better than previously. It should also be mentioned that the doublet is caused by two separate vibrational modes, one (750 cm^{-1}) being the out-of-plane C-H ring deformation of a monosubstituted benzene ring, the other (780 cm^{-1}) that of a meta-disubstituted benzene ring. These--and all the other bands--are consistent with a structure of 5P4E, consisting of five phenyl rings linked by oxygen bridges, which are attached "meta" to one another. A simple way of accounting for the change of appearance with increased speed is by increased broadening of both the 750 and the 780 cm^{-1} bands. The broadening need not be equal for both components. The region most strongly overlapped by both bands becomes the peak. The broadening could be the result of increased film thickness, film temperature, or both. This change is an illustration that bands consisting of overlapping components are not well suited for temperature determinations from their intensity.

The polarized spectra of Figs. 11b and c are much more different from one another than the unpolarized ones of Figs. 11a. If we compare the major features only, the change of relative intensities of the band structures around 980 and 1150 cm^{-1} with direction of the polarization plane is most outstanding. In the spectra of Fig. 11b the latter band is more intense, in Fig. 11c the former. There are also some changes with speed, but they are more difficult to identify.

The spectra of Fig. 12 are analogous to those of Fig. 11 except for twice the load or contact pressure. The unpolarized spectra are little affected by speed. Again a change takes place in the 750/780 cm^{-1} doublet, but this time the process of band widening and overlap has progressed only to the stage where the dip between the peaks has become less pronounced; it has not yet grown into a peak. However, in either of the unpolarized spectra the 1150 cm^{-1} band structure is more intense than that around 980 cm^{-1}, which is opposite to the behavior at low pressure (Figs. 12a vs. Figs. 11a). Of the polarized spectra, the low speed spectra of Figs. 12b and c still show a 1150 cm^{-1} band more intense than the 990 cm^{-1} band for one direction of polarization and the opposite for the other direction of polarization, as can be seen for the low load spectra of Fig. 11b and c, but the ratio of these two band intensities is not affected by polarization at high speed and high load.

Polarization effects must be due to preferred alignment of the lubricant molecules since the instrumentation is cylindrically symmetrical about the optical axis (except for the beam splitter and the flat mirrors, but that effect is quite small). Shear rate, adsorption, a temperature gradient, solidification, could provide such a preferred direction. Variation of the operating parameters in a precise manner and study of the corresponding changes in different emission bands will permit an identification of the most important factors involved.

It might seem strange that the difference between spectra obtained at the two orthogonal polarization planes was less at high pressure than at low pressure. Since polarization differences are indicative of molecular alignment, high pressures should favor directional alignment. Pictorially, chain-like molecules can be considered as resembling spaghetti. As they pass through the ehd contact, they become "aligned", i.e. neighboring noodles are oriented parallel to one another. Since infrared spectral bands are caused by vibrations between atoms

or groups of atoms in a molecule, molecular alignment is reflected by spectral polarization. If the molecules were randomly oriented, changing of the plane of polarization in the spectrometer would not influence the spectrum. Since increased pressure reduces polarization, it must promote random molecular orientation. Conceptually, this could happen by "curling up" of the molecular chains. The molecular chains become "kinked" and form balls. Now the molecules are randomly oriented with respect to any direction of view.

This picture is not very different from the one derived for some of the n-alkanes by Schnur's[7] group at the Naval Research Laboratory. Raman spectroscopy was used on samples maintained at high pressures in a diamond anvil cell. The high pressure Raman spectrum of heptane showed a drop in the intensities of acoustic bands between 300 and 600 cm^{-1} indicating a decrease in the molecular population with all trans conformers and one gauche bond in favor of more highly kinked conformers. Furthermore, the high-frequency spectrum of heptane lacked a sharp peak at near 2800 cm^{-1}, which showed a reduction in lateral chain order. The primary conclusion of this work has been summarized in a recent theoretical paper by these authors[8]. It states "that for relatively short chains, at least as long as hexadecane, an increase in pressure causes an increase in the number of gauche bonds, i.e. the molecules become more globular in character".

Polyphenyl ether is a chain, not of methylene, but of phenyl groups. However, similar reasoning should also apply. This theory, if found applicable to our situation, could be extended to include viscosities and tractions for various molecular structures. A preliminary theoretical effort is planned for the near future.

Table I gives the assignments of the principal infrared bands of 5P4E polyphenyl ether according to Randle and Whiffen[9]. Only the monosubstituted and meta-disubstituted assignments are in line with observations, so that our fluid consists primarily of meta-connected benzene rings.

4.2 Some Experiments with Monsanto Traction Fluid Sanotrac P-40

This fluid is one of the commercial fluids of the Monsanto Company. Its grating absorption spectrum is shown in Fig. 13.

In our ehd apparatus some peculiar behavior was noticed. At low sliding speed the interferogram showed periodic ups and downs (period: about four minutes). At the same time, changes of fluid flow pattern were observed on the ball. At the ball circumference in contact with the diamond, more and more fluid would accumulate forming a ridge or a dromedary-like hump. Then the hump would collapse. After a while it would start growing again. The changes of the level in the interferogram correspond to temperature changes of perhaps $0.1^{o}C$. When the pressure on the ball was increased, the periodicity would remain the same but the amplitudes would reduce. The contact could not have been starved at any time, for the temperature swings were too small for that.

Spectra calculated from these interferograms are shown in Figs. 14 and 15. The band near 690 cm^{-1} was not present in the low load spectrum, which had the more pronounced cyclic behavior.

The phenomenon resembled a winding up process, followed by collapse. After a few days of experimenting with this fluid, our motor burnt out. The traction was too much for it! It has since been replaced.

4.3 Infrared Analysis of Polyethylene Wear Specimens Using Attenuated Total Reflection Spectroscopy

4.3.1 Results

Three samples of ultrahigh molecular weight polyethylene wear specimens,

all in the form of a short cylinder of about 10mm diameter with a hemispherical end by Mr. Jones and sent to us for surface analysis. The rubbed flats at the hemispherical end were only about 3mm in diameter.

Our task was to look for possible oxidation or unsaturation at the rubbed surface by comparing its ATR spectra with those of other parts of the specimens. ATR infrared spectroscopy is not a simple technique, at best (surface areas of about 6 cm^2, allowing more than 10 reflection on either side of the crystal plate) so that the small rubbed area (about 0.1 cm^2) required the utmost care.

The procedure chosen was the following: One 100 μm thick slice was cut from the worn end (3mm diameter) and three 100 μm thick slices from the opposite end (discarding the extreme end, except for one of the samples) with a precision biological microtome. The cutting was done very slowly. The slices were cleaned with water and detergent, then rinsed with distilled water, then with alcohol, and then with pentane and dried. Then the slices -- or slice from the worn surface -- were placed on a well-cleaned germanium ATR plate in such a way that the outer surfaces faced the plate. The slice with the worn face was put alone on the plate but -- except for one run with the other end surface alone -- three full-diameter slices were placed on one side of the plate together, like pancakes on a griddle. For this reason the absorption bands of the references were always stronger than those of the rubbed surfaces.

The infrared spectrum for the unworn end of the 5mRad irradiated specimen appears in figure 16a. The surface facing the germanium plate was the flat, unworn end of the rider specimen. The procedure for removal of moisture and carbon dioxide was effective as evidenced by the lack of fine structure in the 1400 to 1800 cm^{-1} region. The most intense bands are at 2851 and 2919 cm^{-1} (C-H stretching), 1460 cm^{-1} (C-H deformation), and at 827 and 741 cm^{-1} (CH_2 rocking). These are bands that would be expected for a polyethylene surface[10].

There is a slight indication of a band at 1743 cm^{-1}, which would indicate the presence of carbonyl, but it is very weak. The spectrum of the wear scar surface for the 5mRad specimen is shown in Fig. 16b. This spectrum is identical to the one for the unworn surface (Fig.16a) with two exceptions. There is no indication of a band at 1743 cm^{-1} and a weak broad band is present from 3100 to 3300 cm^{-1}. This weak band probably is due to a small amount of moisture adsorbed on the surface.

The infrared spectra of the wear scar surface and the polymer interior for the 2.5mRad specimen appear in Figs. 18a and b, respectively. Again, these spectra appear identical. Both have the broad weak band centered at 3100 cm^{-1} and the other bands associated with polyethylene.

Fig.19 contains the corresponding spectra for the unirradiated polymer. The spectrum for the wear scar surface appears in Fig. 19a and the spectrum for the polymer interior in Fig. 19b. Both spectra are essentially the same and very similar to the spectra for the two irradiated specimens.

4.3.2 Interpretation

The ATR spectrum is of the nature of a surface absorption spectrum. The intensity of the bands is a function of the "effective optical path" and is strongly dependent on the angle of incidence on the plate and sample. Multiple reflections build up the band intensities. However, as previously mentioned, only one reflection could be used for the wear surface and three for the bulk polymer because of size limitations. Accordingly, the intensities of the spectral bands are necessarily weak.

Taking this into account, there does not appear to be any significant polymer surface degradation (oxidation or unsaturation) resulting from either

the irradiation procedure or the friction and wear process. It would follow that the surface adsorption characteristics of the irradiated polyethylene should not be grossly different from those for the virgin polymer.

Since the boundary lubricating characteristics are highly dependent on the adsorption of polar molecules onto the polymer surface, one would not expect gross differences in these characteristics either.

4.3.3 Summary of results

Attenuated total reflection infrared spectroscopy was used to analyze ultrahigh molecular weight polyethylene wear test specimens. The following results were obtained:

1) Neither gamma sterilization irradiation (to 5.0mRad) nor the friction and wear process itself produced any substantial amount of polymer surface degradation.
2) The only spectral band detected on most of the polymer surfaces and not related to the polyethylene itself was a broad weak band centered at 3100 cm^{-1}. This was probably the result of a small amount of adsorbed moisture.
3) Therefore, it was concluded that the sterilization process should not alter the boundary lubricating properties of the polyethylene.

REFERENCES

1. Lauer, J.L., Study of Dynamic Emission Spectra from Lubricant Films in an Elastohydrodynamic Contact Using Infrared Fourier Transform Spectroscopy. NASA CR-159418, August 28, 1978.
2. Viskanta, R., and Anderson, E.E., "Heat Transfer in Semitransparent Solids", in "Advances in Heat Transfer" (T.F. Irvine, Jr., and J.P. Hartnett, Editors). Vol. 11. Academic Press, New York 1975, pp. 317-341.
3. Chandrasekhar, S., "Radiative Transfer", Arnold Constable Ltd., London, 1950.
4. Griffith, P.R., "Chemical Infrared Fourier Transform Spectroscopy". John Wiley & Sons, New York, 1975, pp. 40-44.
5. Rakov, A.V., Optika i Spectr. 7, 202 (1959).
6. Huong, P.V., "Infrared Emission Spectroscopy," in Advances in Infrared and Raman Spectroscopy, Vol. 4 (R.J.H. Clark and R.E. Hester, Editors), pp. 90-92, Heyden Publishing Co., London 1978.
7. Schoen, P.E., Priest, R.G., Sheridan, J.P., and Schnur, J.M., "Pressure-induced Changes in Molecular Conformation in Liquid Alkanes". Nature, 270, 412-414 (1977).
8. Schoen, P.E., Priest, R.G., Sheridan, J.P., and Schnur, J.M., "Pressure-induced Changes in Liquid Alkane Chain Conformations". Submitted for publication in J. Chem. Phys. 1979.
9. Randle, R.R., and Whiffen, D.H., Molecular Spectroscopy, Conference held by The Institute of Petroleum, London (1954), Published by The Institute of Petroleum, pp. 111-128 (1955).
10. Aggarwal, S.L., and Swecting, O.J., Chem. Revs., 57, 665 (1957) and references therein.

APPENDIX I

PRESENTATIONS AND PUBLICATIONS IN 1978

1. "Polarized Infrared Emission Spectra from Operating Bearings." Paper No. 592. Invited paper presented at the Coblentz Symposium of the 29th Pittsburgh Conference at Cleveland, Ohio, on March 1, 1978.
2. "Chemistry and Physics of Lubricants." One-hour invited lecture at Session III--Lubricants, Manufacturing of Wire III, Clinic, Society of Manufacturing Engineers, April 5, 1978, in Newark, N.J. Paper for publication Wire World was invited.
3. "Study of Polyphenyl Ether Fluid (5P4E) in Operating Elastohydrodynamic Contacts by Infrared Emission Spectroscopy." Presented at the ASLE/ASME Joint Lubrication Conference in Minneapolis on October 25, 1978 (Paper No. 78 - Lub-21). (Published in J. of Lubrication Technology, 101, 67 (1979).)
4. "High-Pressure Infrared Interferometry" in Fourier Transform Infrared Spectroscopy, Vol. 1, Chapter 5, pp. 169-213, Academic Press, N.Y. 1978.
5. "Traction and Lubricant Film Temperature as Related to the Glass Transition Temperature and Solidification." ASLE Transactions, Vol. 21, 250-256 (July 1978).
6. "Orientation of Lubricant Molecules in Operating Bearings by Polarized Infrared Fourier Microspectroscopy" (Paper No. 70). Presented at the 25th Canadian Spectroscopy Symposium, Mt-Gabriel, Quebec, Canada, September 29/30, 1978.
7. "Fourier Emission Infrared Microspectrometer for Surface Analysis"(Paper No. 17). Presented at the 25th Canadian Spectroscopy Symposium, Mt-Gabriel, Quebec, Canada, September 28/29, 1978.

APPENDIX II

MATHEMATICAL SYMBOLS

a	Gaussian band parameter
$f(\nu)$	Gaussian emission band contour function
$I_\nu(y,\theta)$	monochromatic intensity at frequency and angle θ with y
$I_b(M)$	radiance of metal surface
$I_{b\nu}(y)$	blackbody radiance at temperature T(y)
I^+	radiance in the outgoing direction from the film
I^-	radiance in the ingoing direction from film
$k=\kappa/\cos\theta$	absorption coefficient
kT	thermal energy
L	film thickness
$n_\nu(y)$	index of refraction of film
t	transmissivity
T	absolute film temperature
U	viscosity barrier potential
y	distance from exit surface of fluid film
β	reflection coefficient defined by Eq. 6
Γ	half-width of Gaussian emission band
$\varepsilon_{1\nu}(\cos\theta)$ $\varepsilon_{2\nu}(\cos\theta)$	spectral emittance in the θ -direction from fluid film at boundary 1 or 2 absorption coefficient
η	viscosity of fluid
θ	ray angle with optic axis
$\kappa_\nu(y)$	absorption coefficient
ν	infrared frequency in cm^{-1}
$\rho_{1\nu}$ $\rho_{2\nu}$	spectral reflectivity at film boundary 1 or 2

σ	Gaussian band parameter
τ_y	optical path length through fluid film thickness y
τ_{Ly}	optical path length through fluid film thickness y

Table I

INFRARED BANDS OF 5P4E

Observed Frequency		Monosubstituted Benzene	Meta-Disubstituted
CM^{-1}	Type	(Randle and Whiffen)	Benzene (Ibid.)
690	ϕ C-C	697±11 (very strong)	690±15 (very strong)
750	γ C-H	751±15 (extremely strong)	------
780	γ C-H	------	782±9 (very strong)
865	γ C-H	------	876±10 (very strong)
990	γ C-H	982±6 (very weak)	999±5 (variable)
1100	β C-H	------	1081±10 (medium strong)
1170	β C-H	1177 (medium strong)	------

Note: ϕ C-C out-of-plane ring deformation

γ C-H out-of-plane C-H deformation

β C-H in-plane C-H deformation

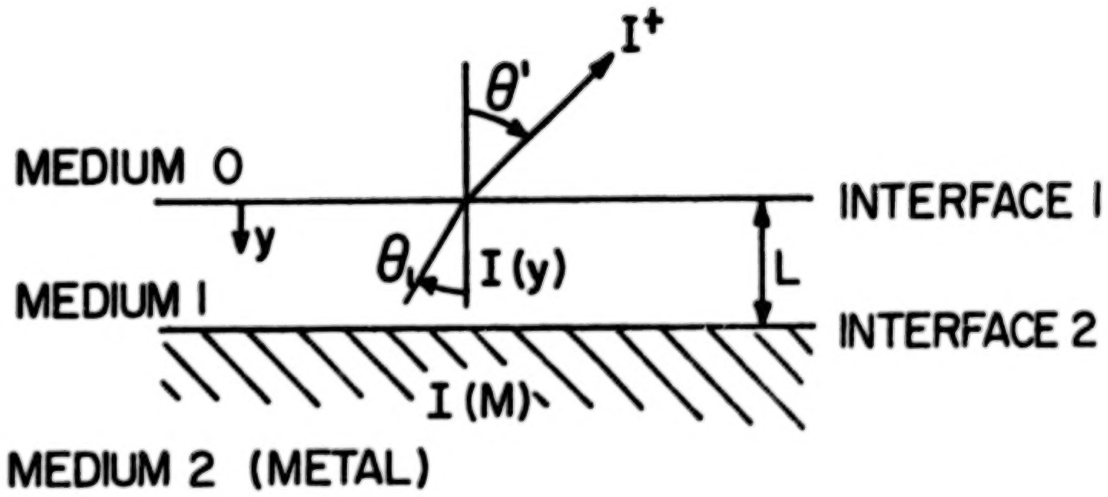

Fig. 1 Schematic diagram of a semi-transparent film on a plate, emitting infrared radiation.

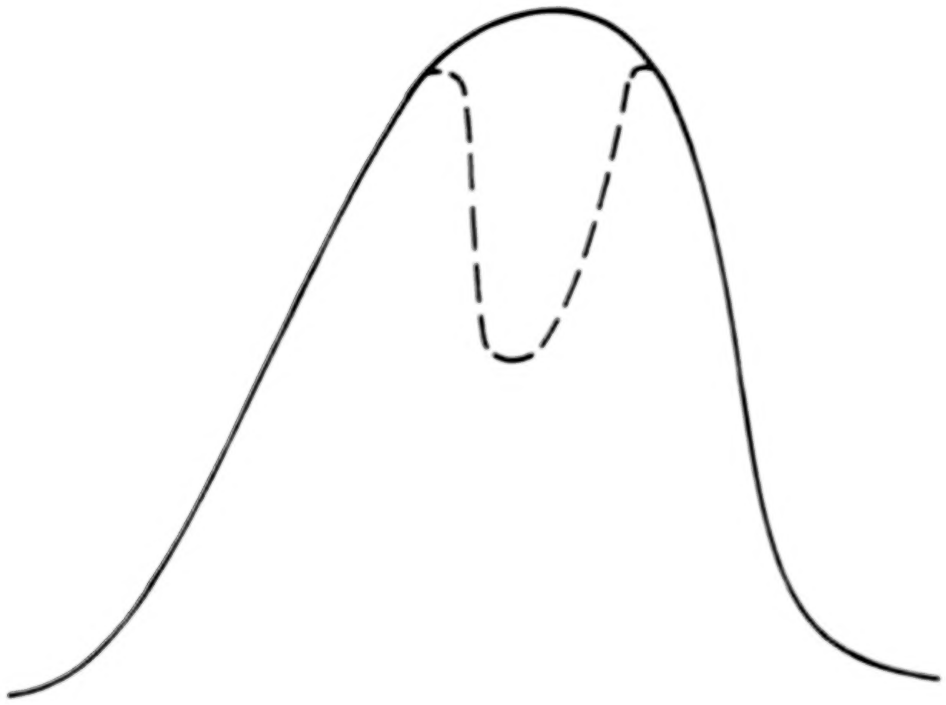

Fig. 2 Infrared emission band showing peak reversal.

BLANK

PAGE

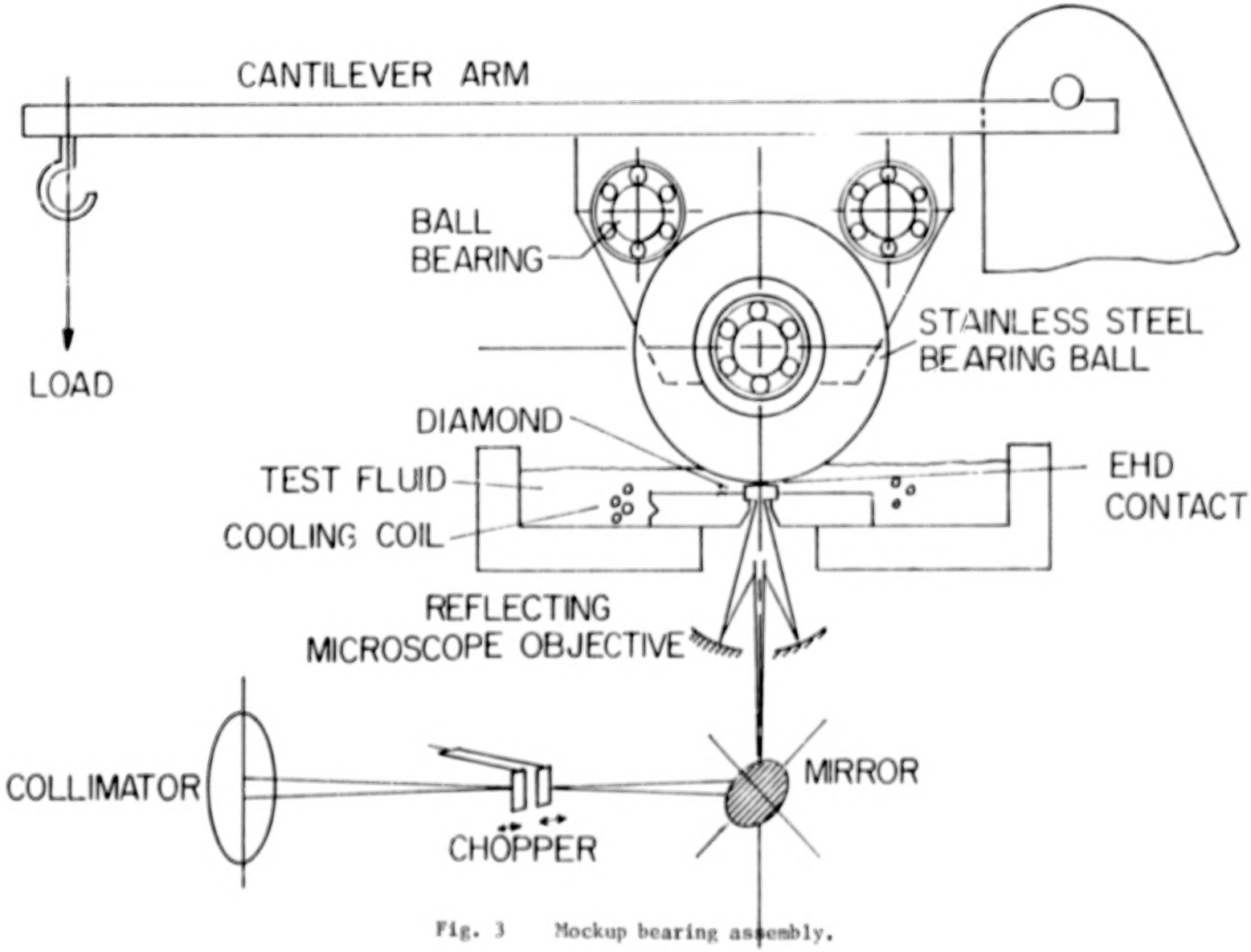

Fig. 3 Mockup bearing assembly.

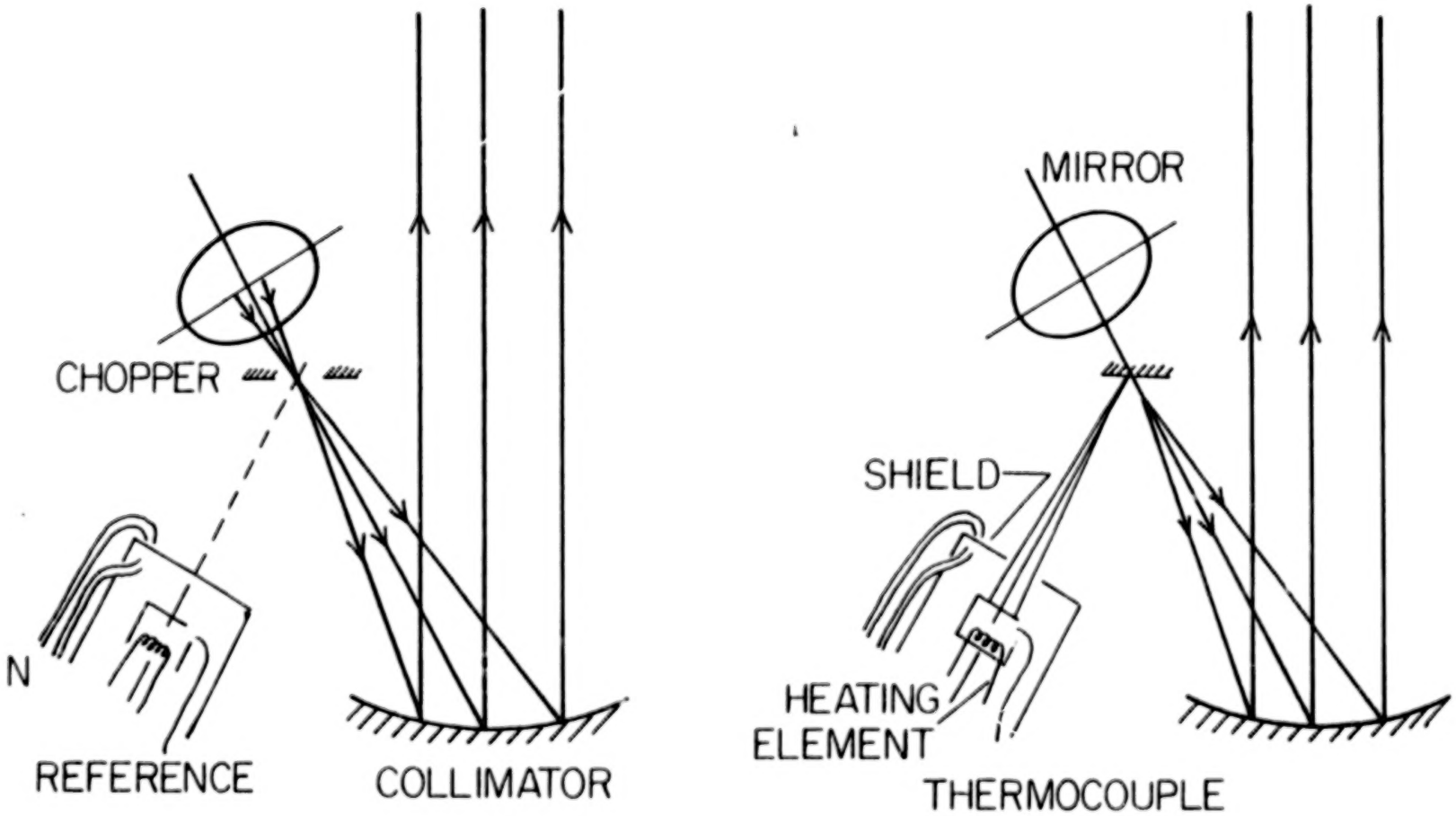

Fig. 4 Chopper and reference assembly.

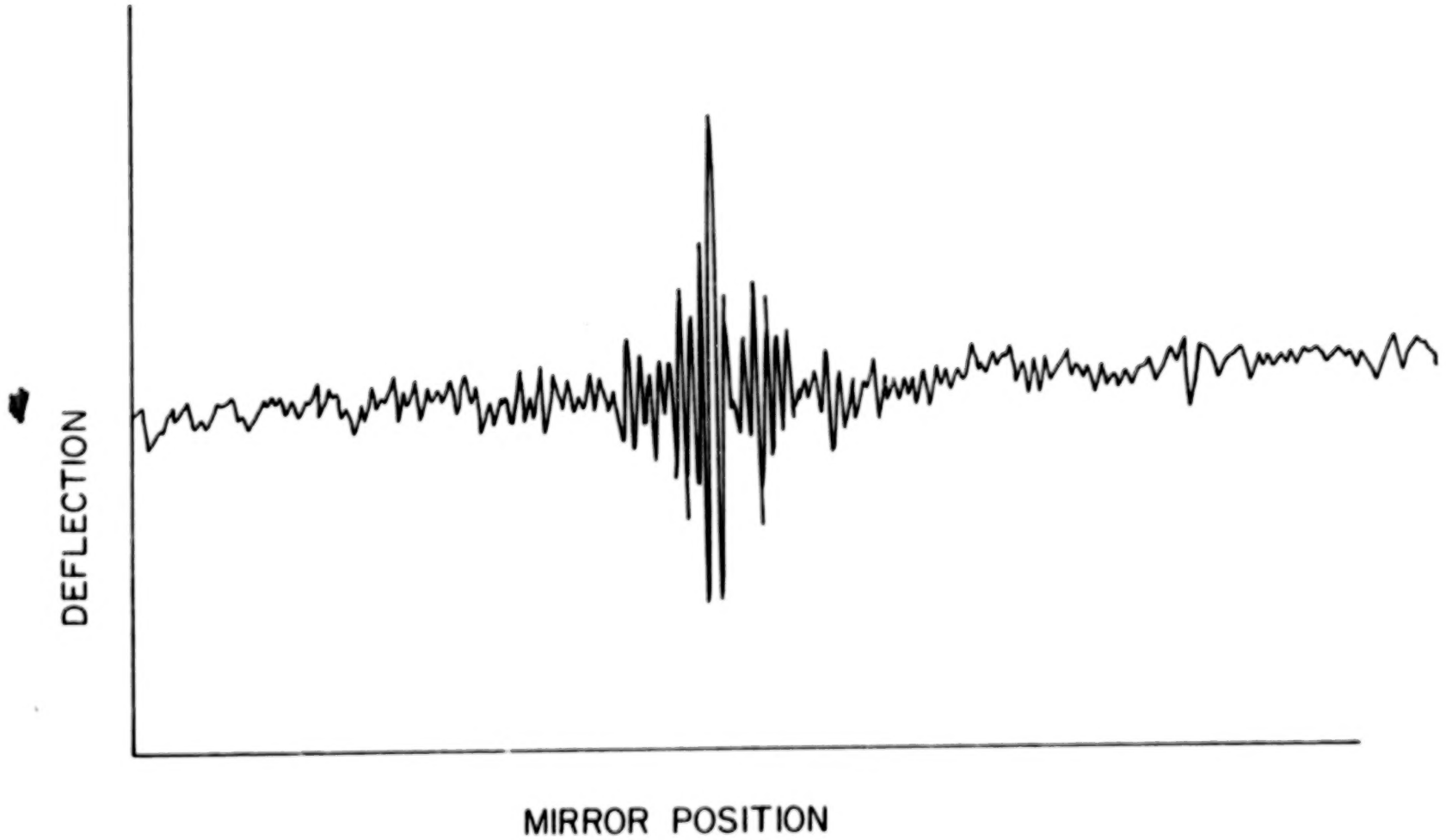

Fig. 5 Interferogram of an emission spectrum from an ehd contact (5P4E, 1 lb. load, 250 RPM) - unfiltered.

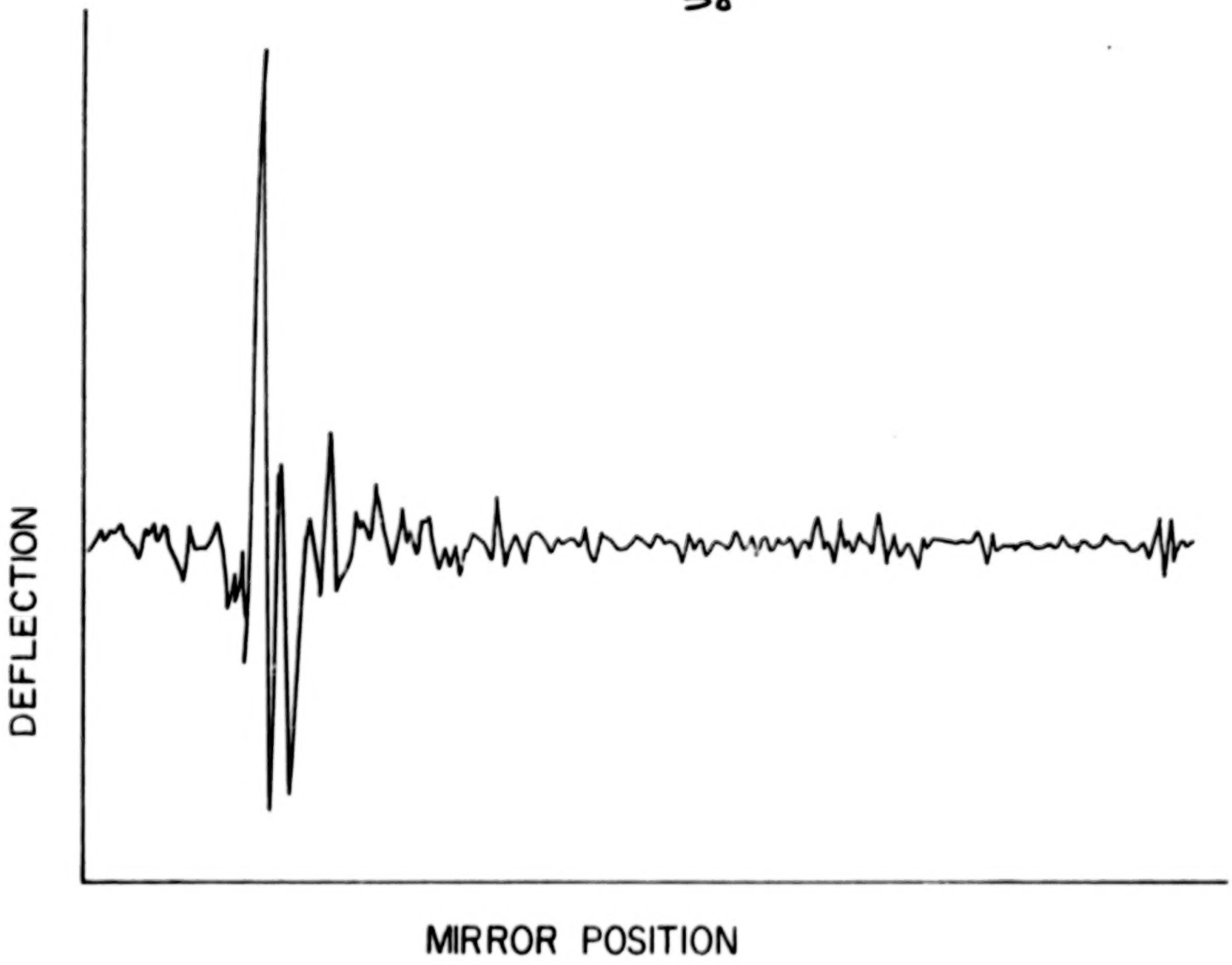

Fig. 6 Interferogram of an emission spectrum from an ehd contact (5P4E, 1 lb. load, 250 RPM) - filtered to include the 630-1230 cm^{-1} spectral region.

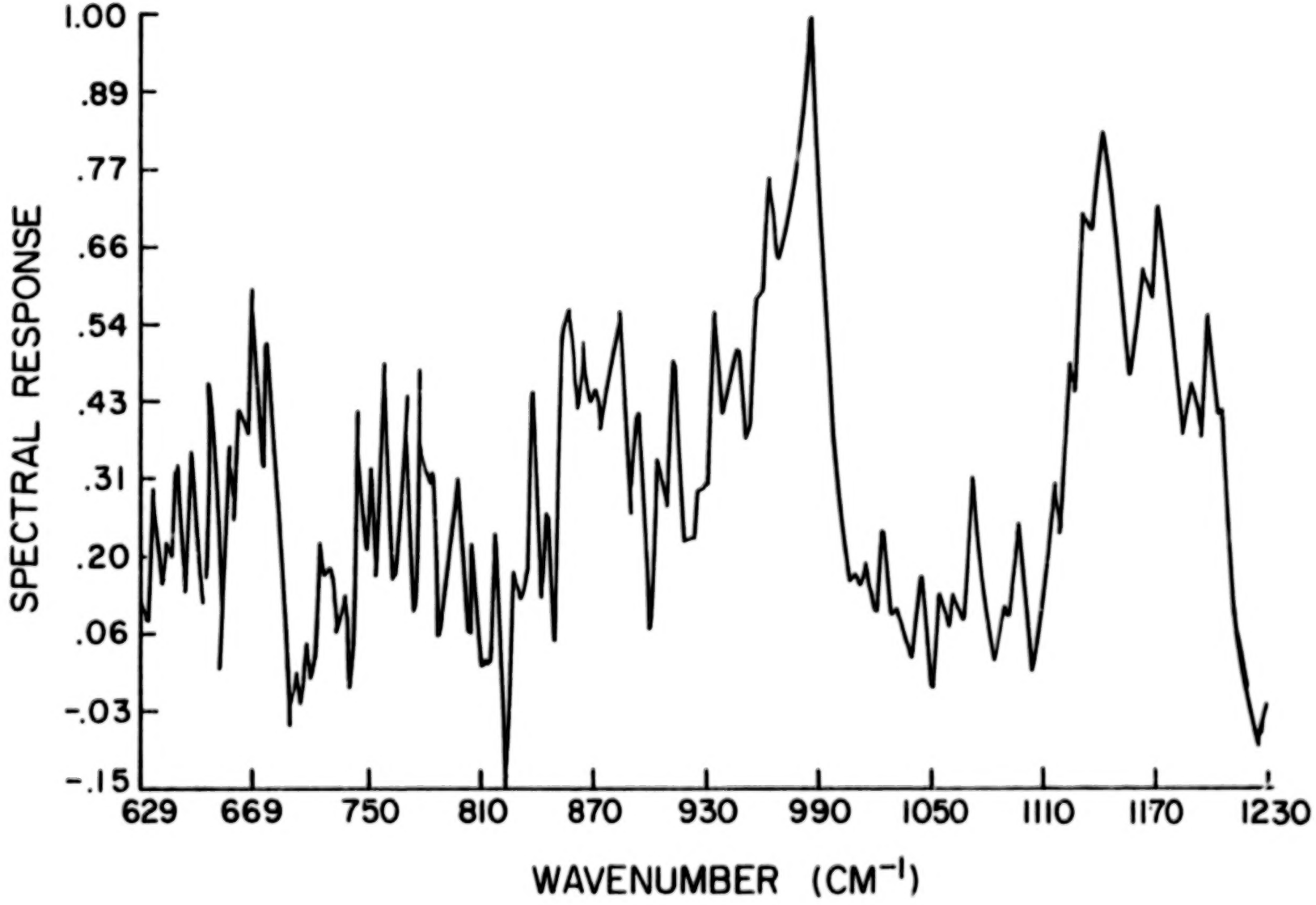

Fig. 7 Spectrum corresponding to Fig. 5 - not smoothed (5P4E, 1 lb. load, 250 RPM).

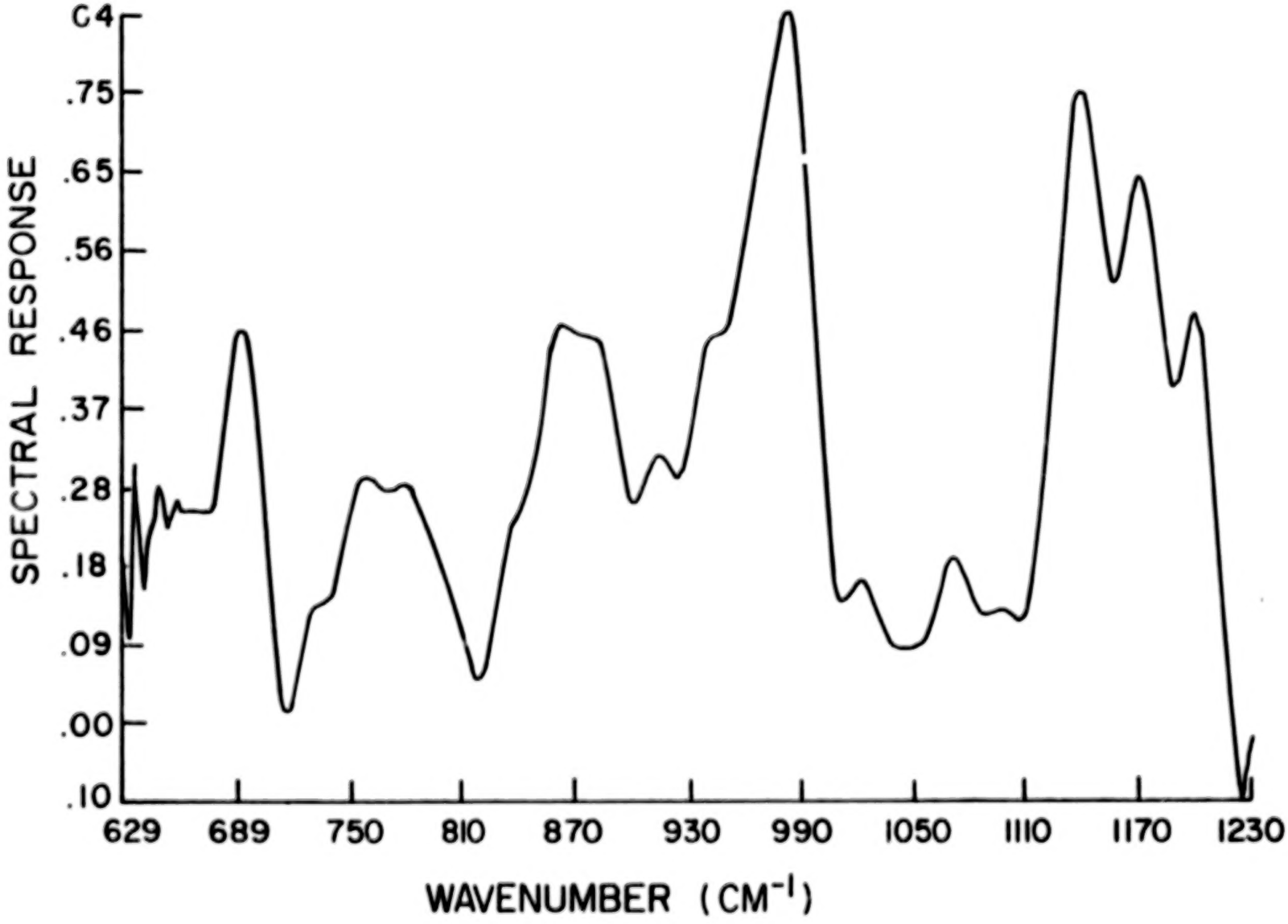

Fig. 8 Spectrum corresponding to Fig. 5 - smoothed (5P4E, 1 lb. load, 250 RPM).

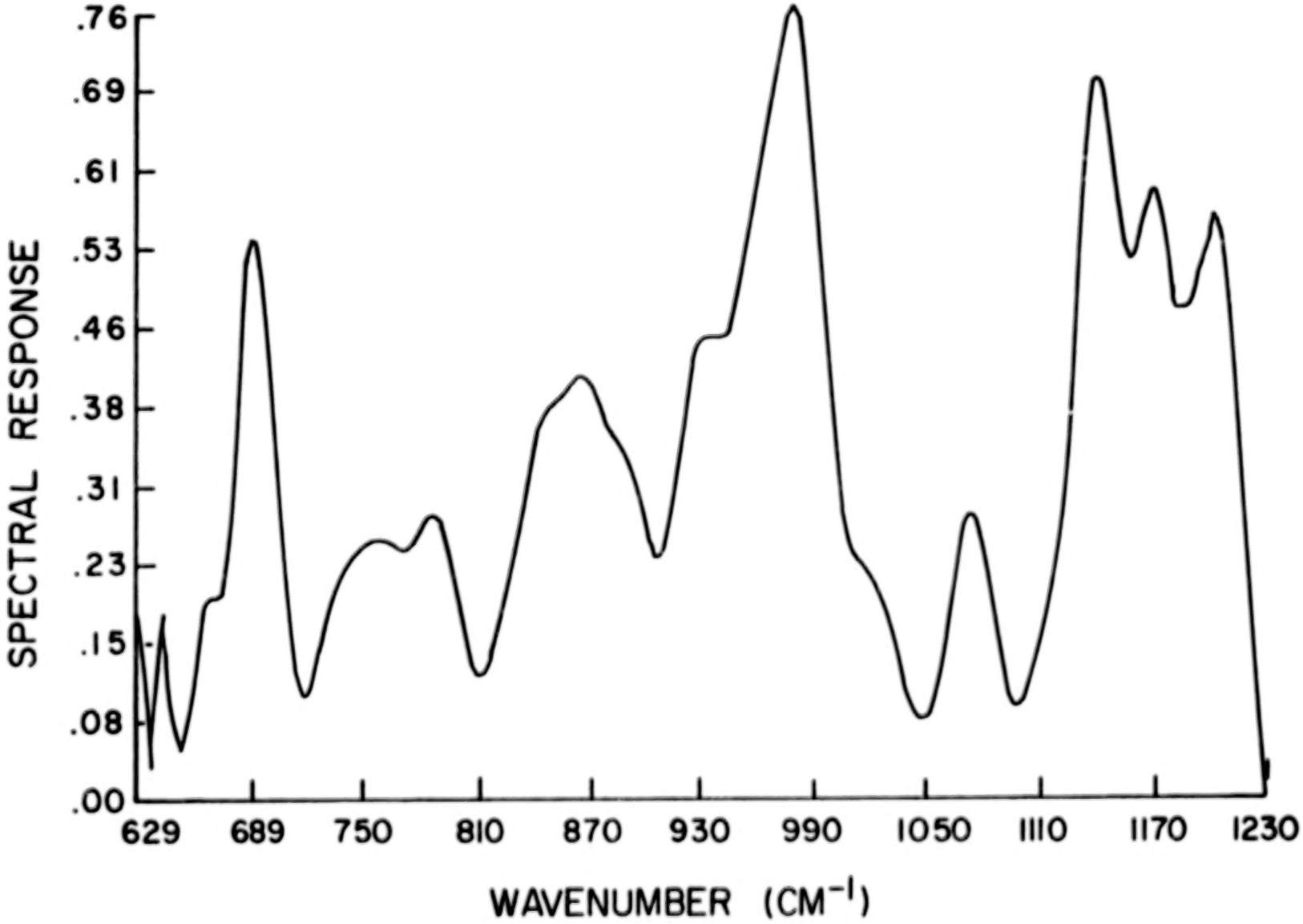

Fig. 9a Emission spectrum of polyphenyl ether fluid (5P4E) from an operating contact, 630 - 1230 cm^{-1}.

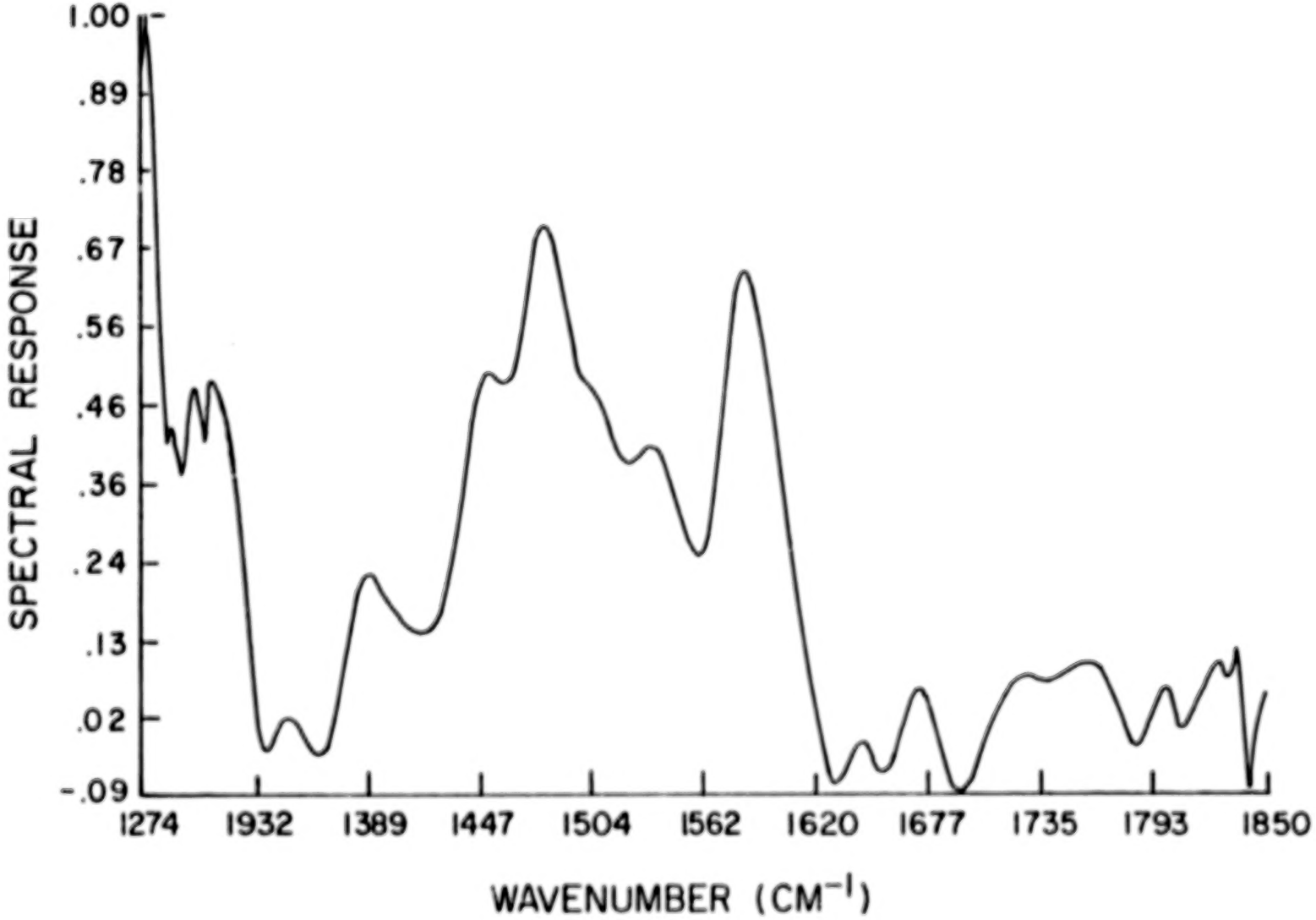

Fig. 9b Emission spectrum of polyphenyl ether fluid (5P4E) from an operating contact, 1275 - 1850 cm^{-1}.

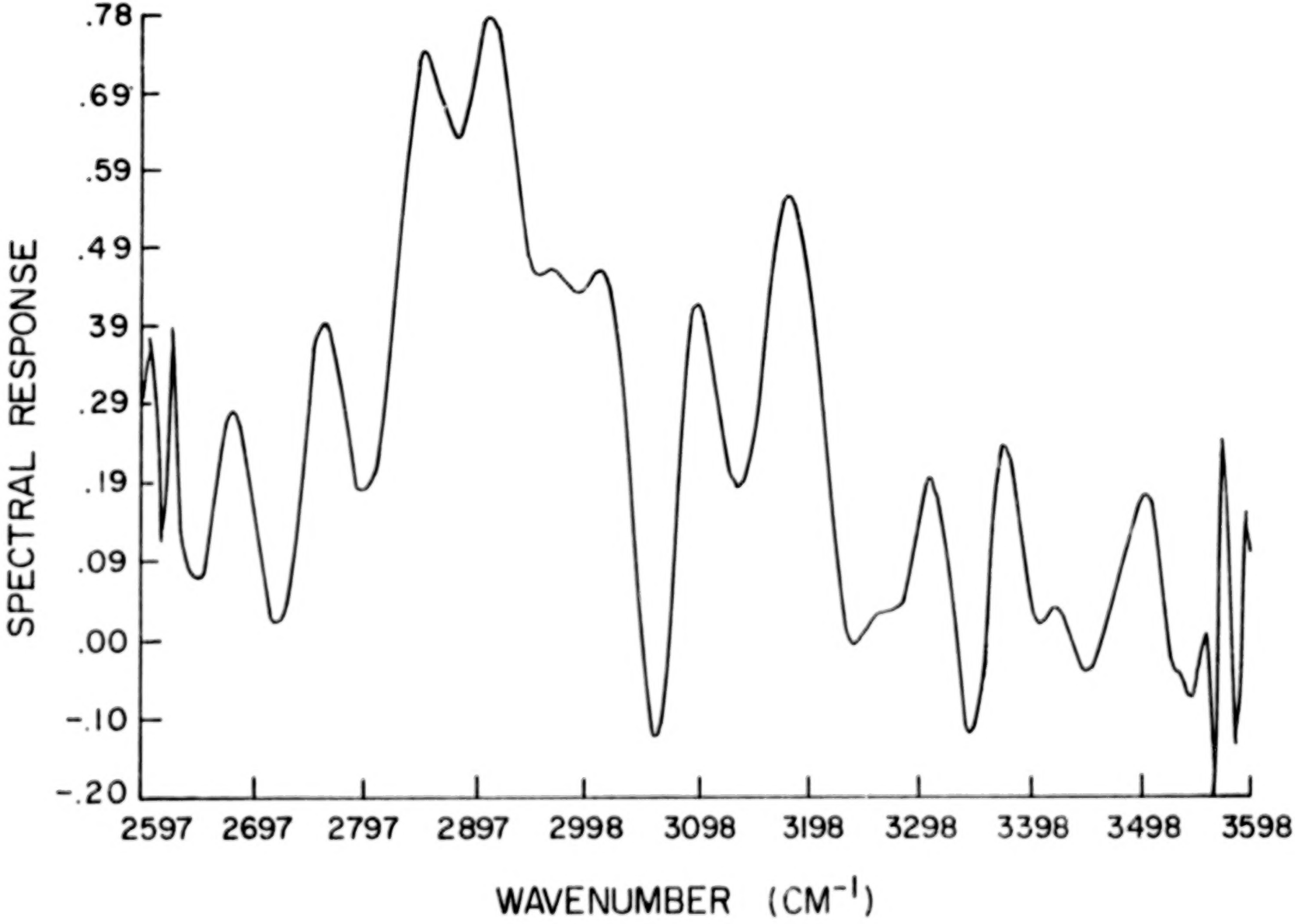

Fig. 9c Emission spectrum of polyphenyl ether fluid (5P4E) from an operating contact, 2600 - 4000 cm^{-1}.

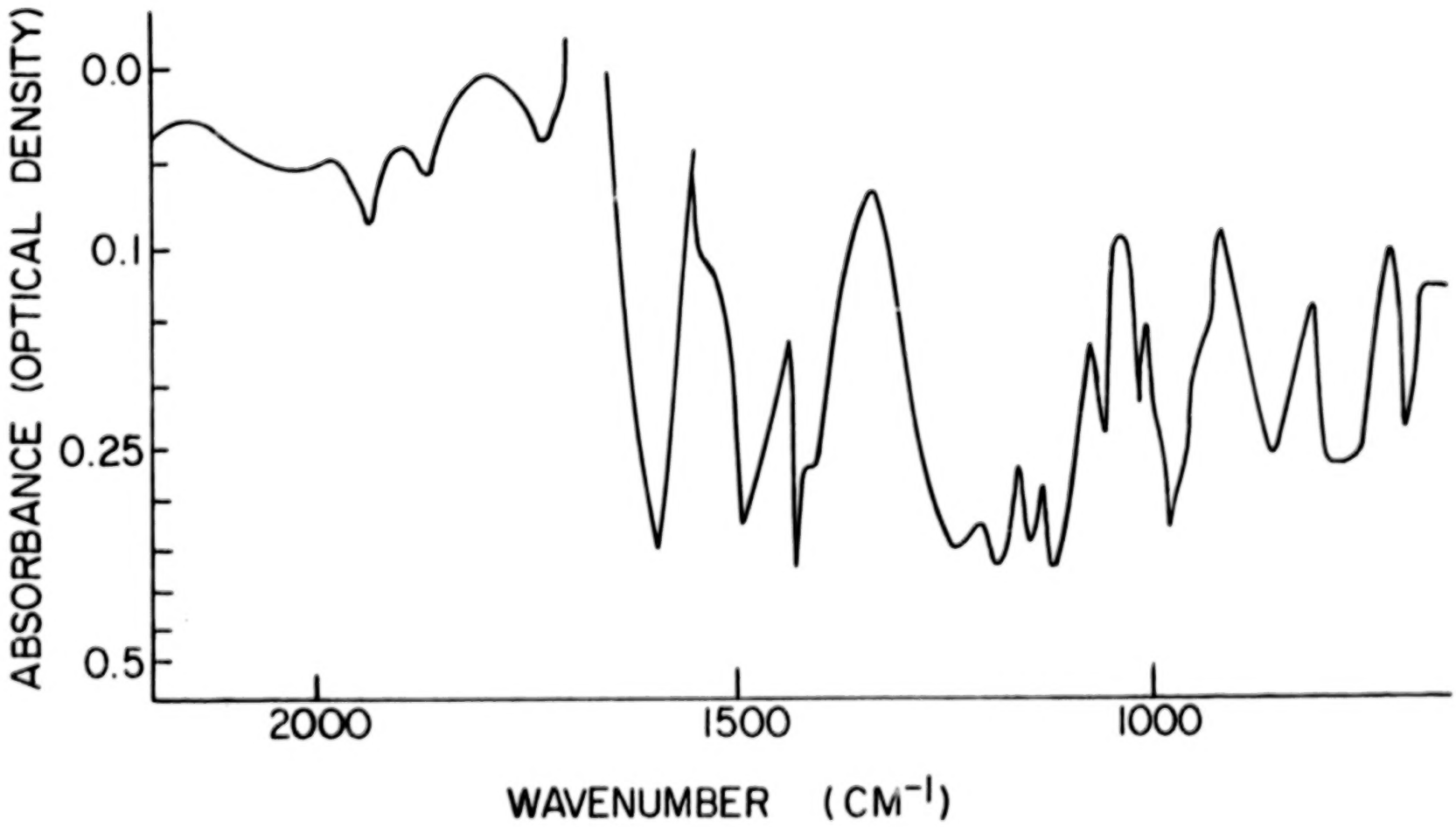

Fig. 10a Absorption spectrum of polyphenyl ether fluid (5P4E) run on a grating spectrometer, 2000 - 3200 cm^{-1}.

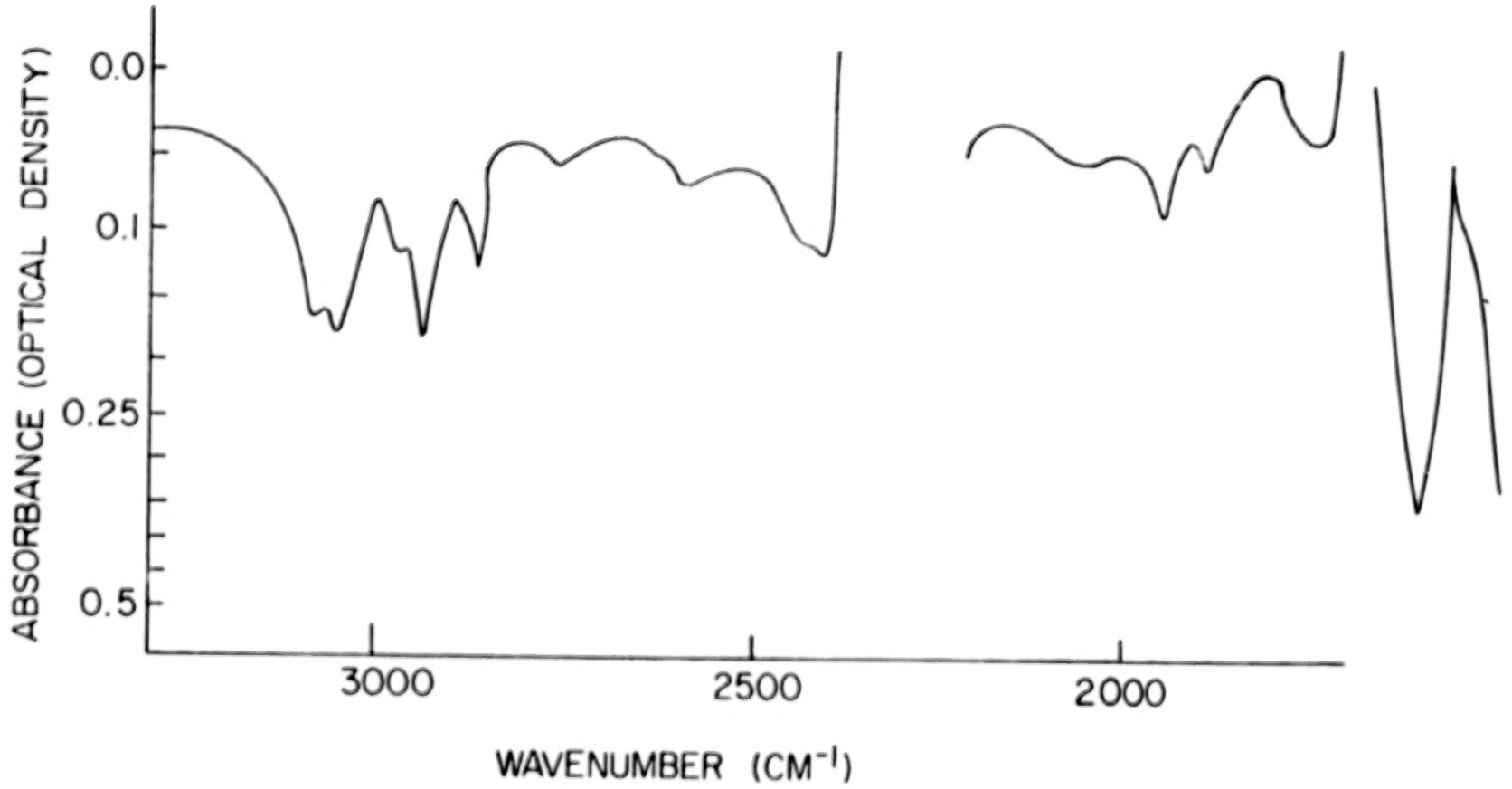

Fig. 10b Absorption spectrum of polyphenyl ether fluid (5P4E) run on a grating spectrometer, 700 - 1700 cm^{-1}.

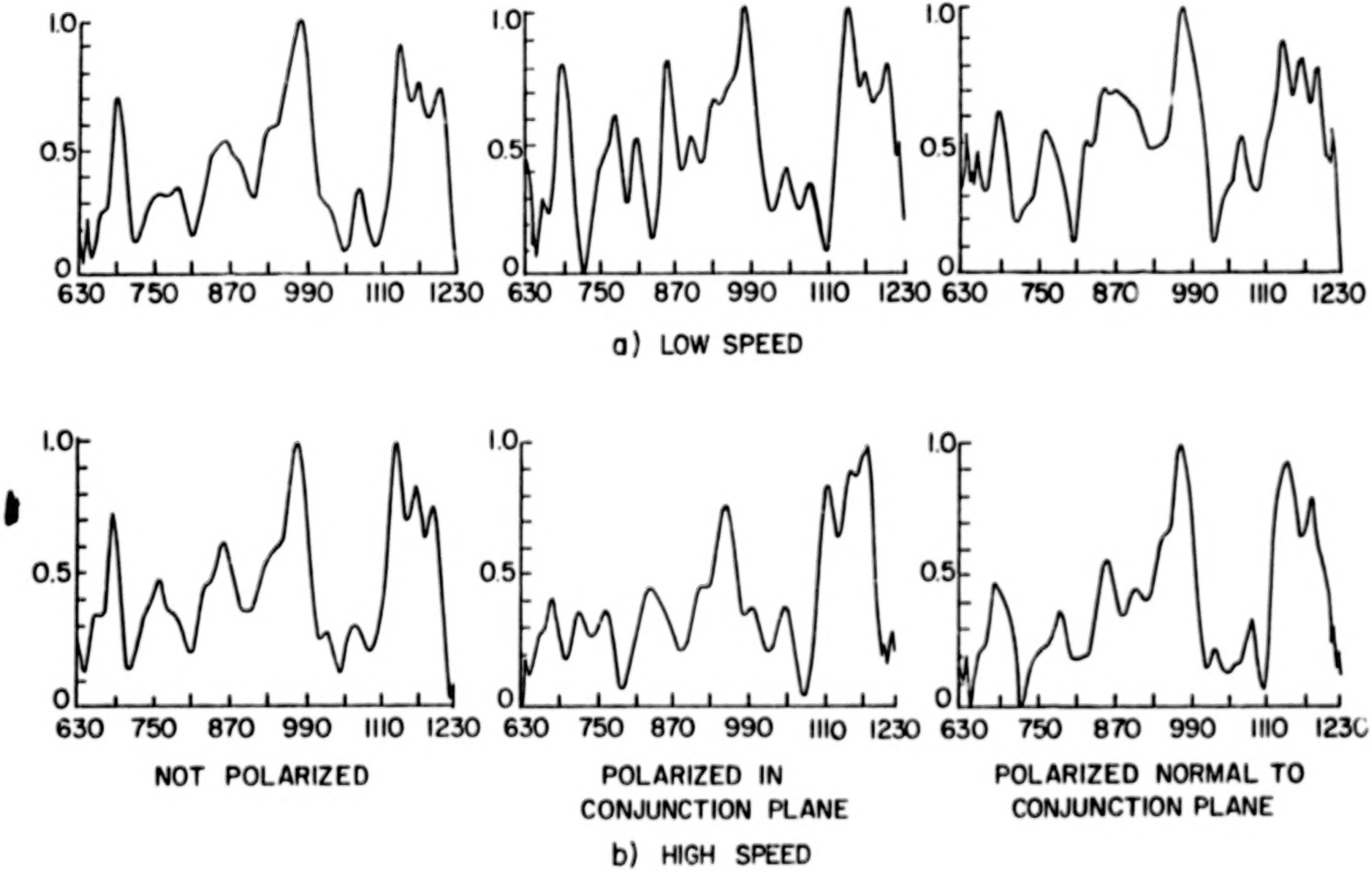

Fig. 11 Emission spectra of polyphenyl ether (5P4E) showing effects of polarization. Average Hertzian pressure 500 MPa, sliding speed of top row 0.7 m/sec, bottom row 1.4 m/sec. The order of the spectra going from left to right is (i) unpolarized, (ii) polarized in the plane of the conjunction line,-and (iii) polarized perpendicularly to the plane of the conjunction line. Abscissas are wavenumbers (cm^{-1}), ordinates are spectral responses.

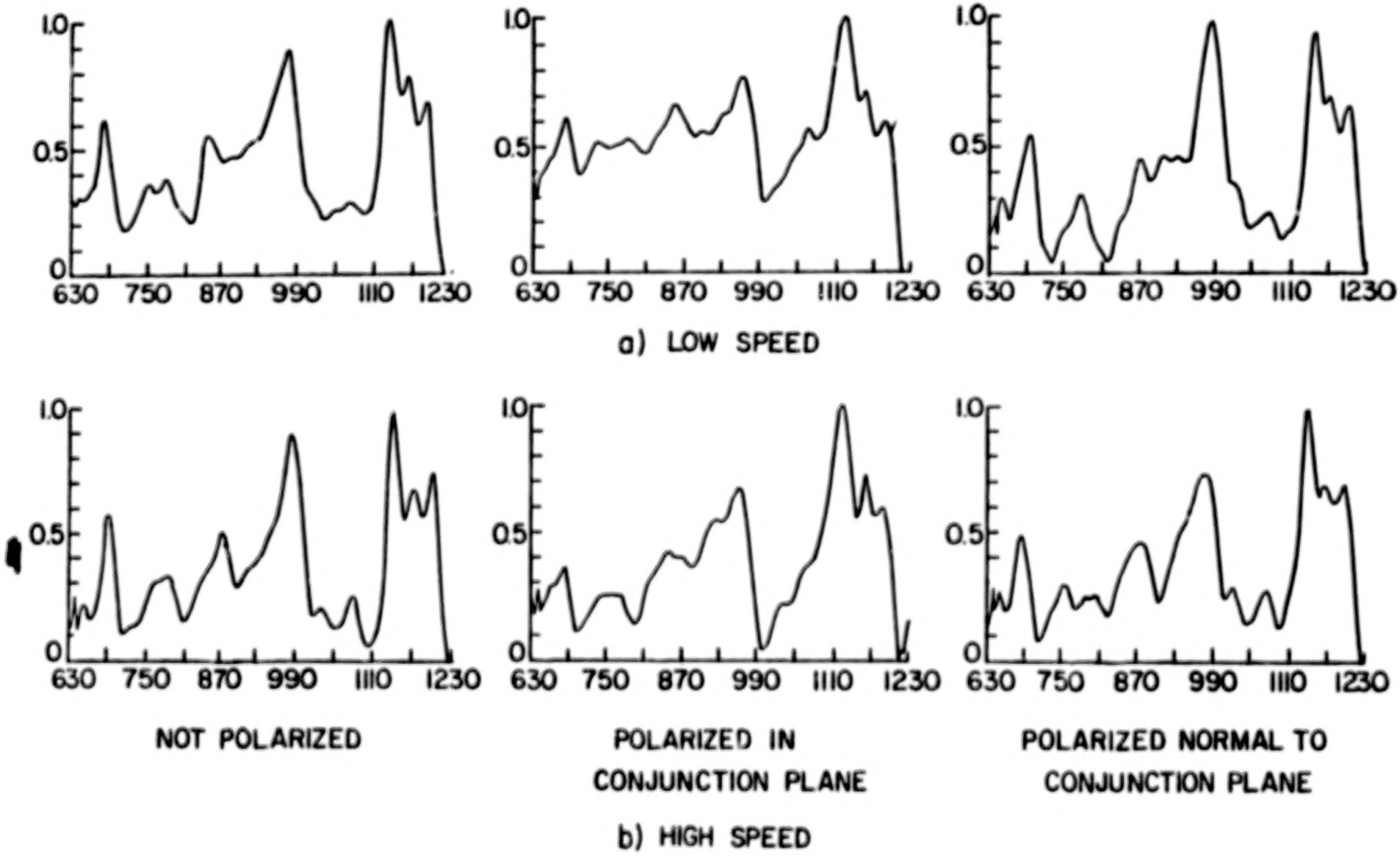

Fig. 12 Emission spectra of polyphenyl ether (5P4E) showing effects of polarization. Average Hertzian pressure 1000 MPa, sliding speed of top row 0.7 m/sec., bottom row 1.4 m/sec. The order of the spectra going from left to right is (i) unpolarized, (ii) polarized in the plane of the conjunction line, and (iii) polarized perpendicularly to the plane of the conjunction line. Abscissas are wavenumbers (cm^{-1}), ordinates are spectral responses.

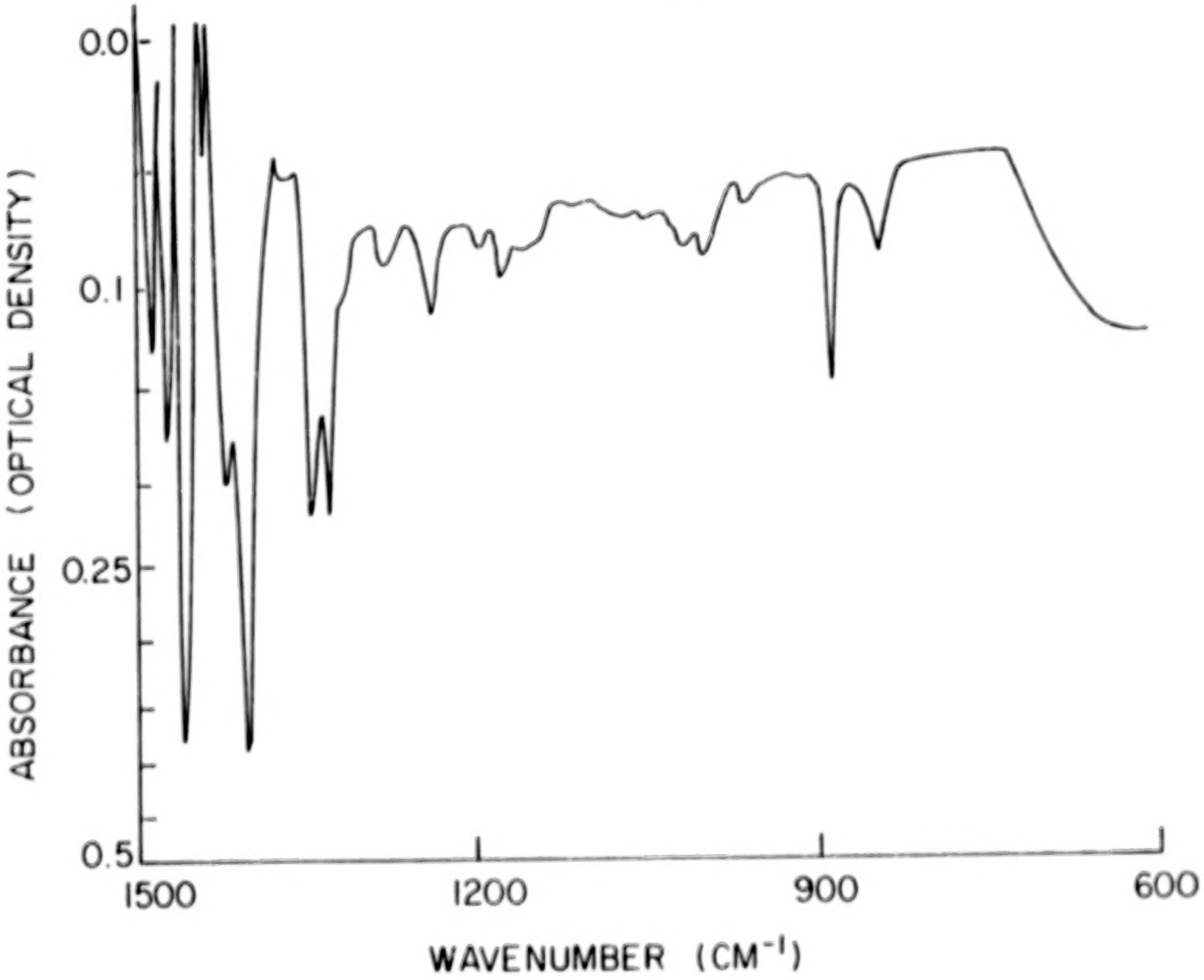

Fig. 13 Absorption spectrum of Monsanto Traction Fluid, Santotrac P-40, run on a grating spectrometer.

Fig. 14 Interferogram of Santotrac P-40, emission from ehd contact, 100 RPM speed, low load (500 MPa average Hertzin pressure) showing periodic fluctuations.

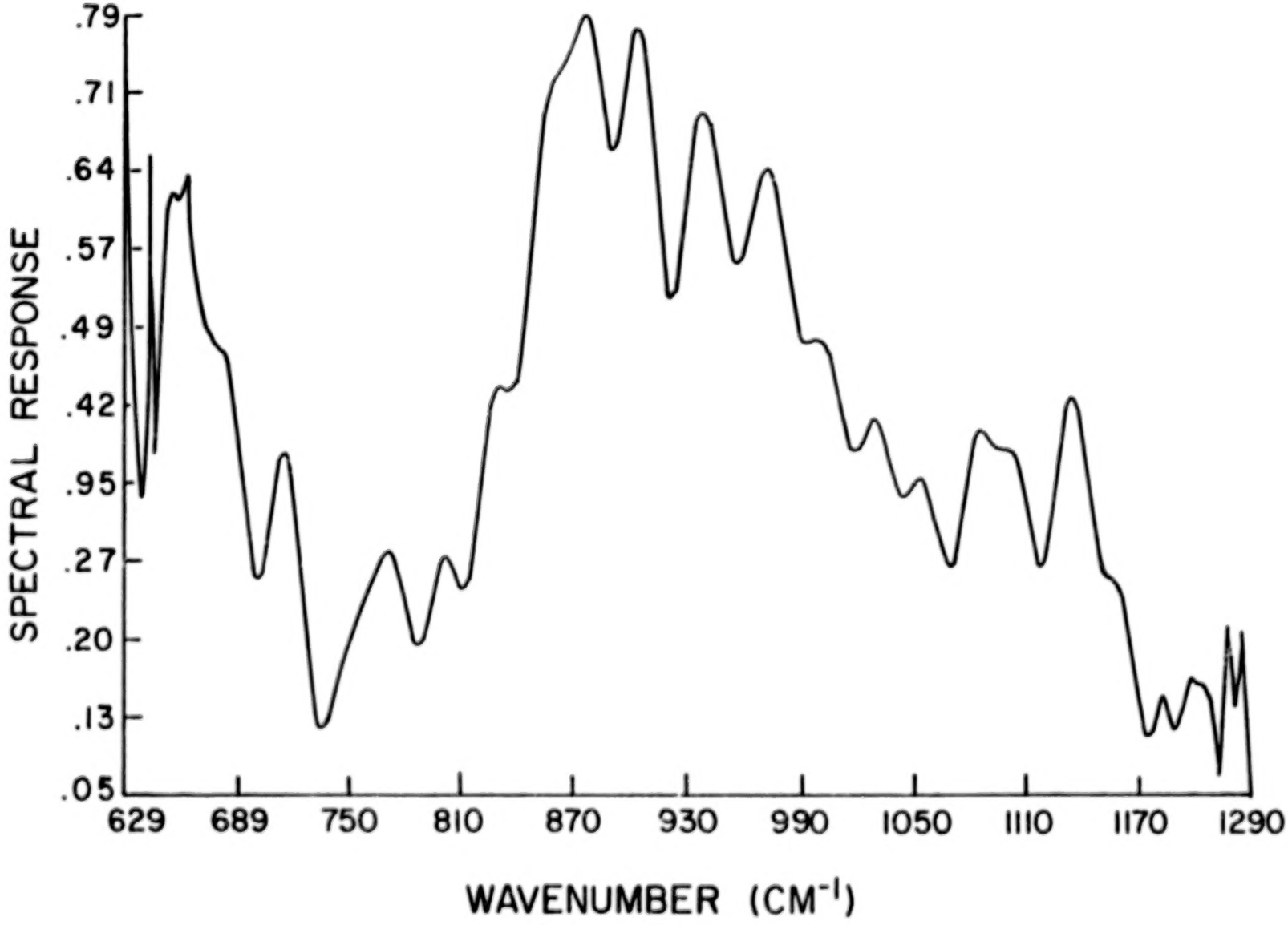

Fig. 15 Ehd emission spectrum of Sanotrac P-40 at low load (500 MPa average Hertzian Pressure) and 100 RPM speed.

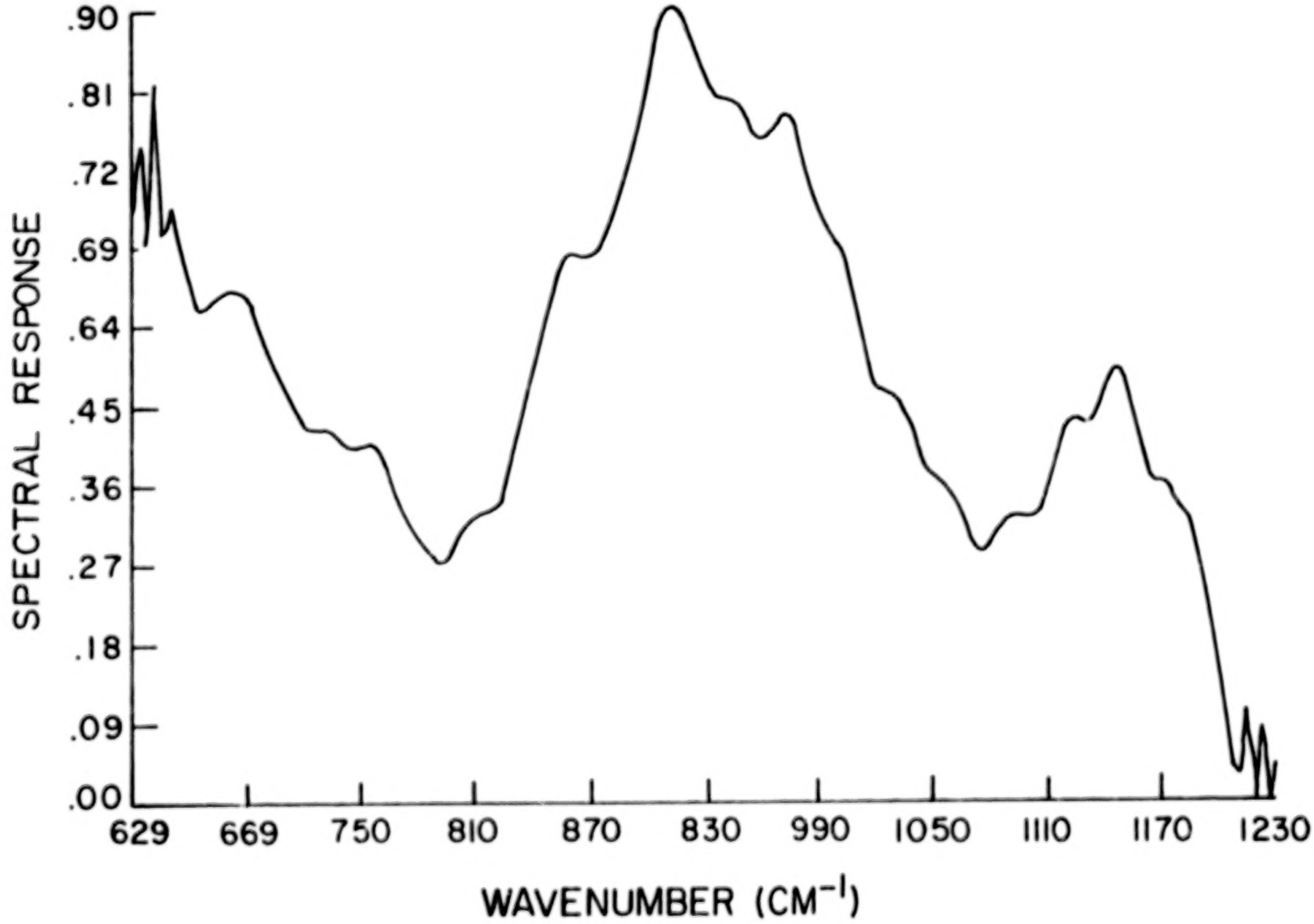

Fig. 16 Ehd emission spectrum of Sanotrac P-40 at 1000 MPa average Hertzian pressure (high load compared to Fig. 15). Note that the 890 cm^{-1} has become much broader and the peak shifted toward higher wave numbers. The spectrum is much smoother than that of Fig. 15.

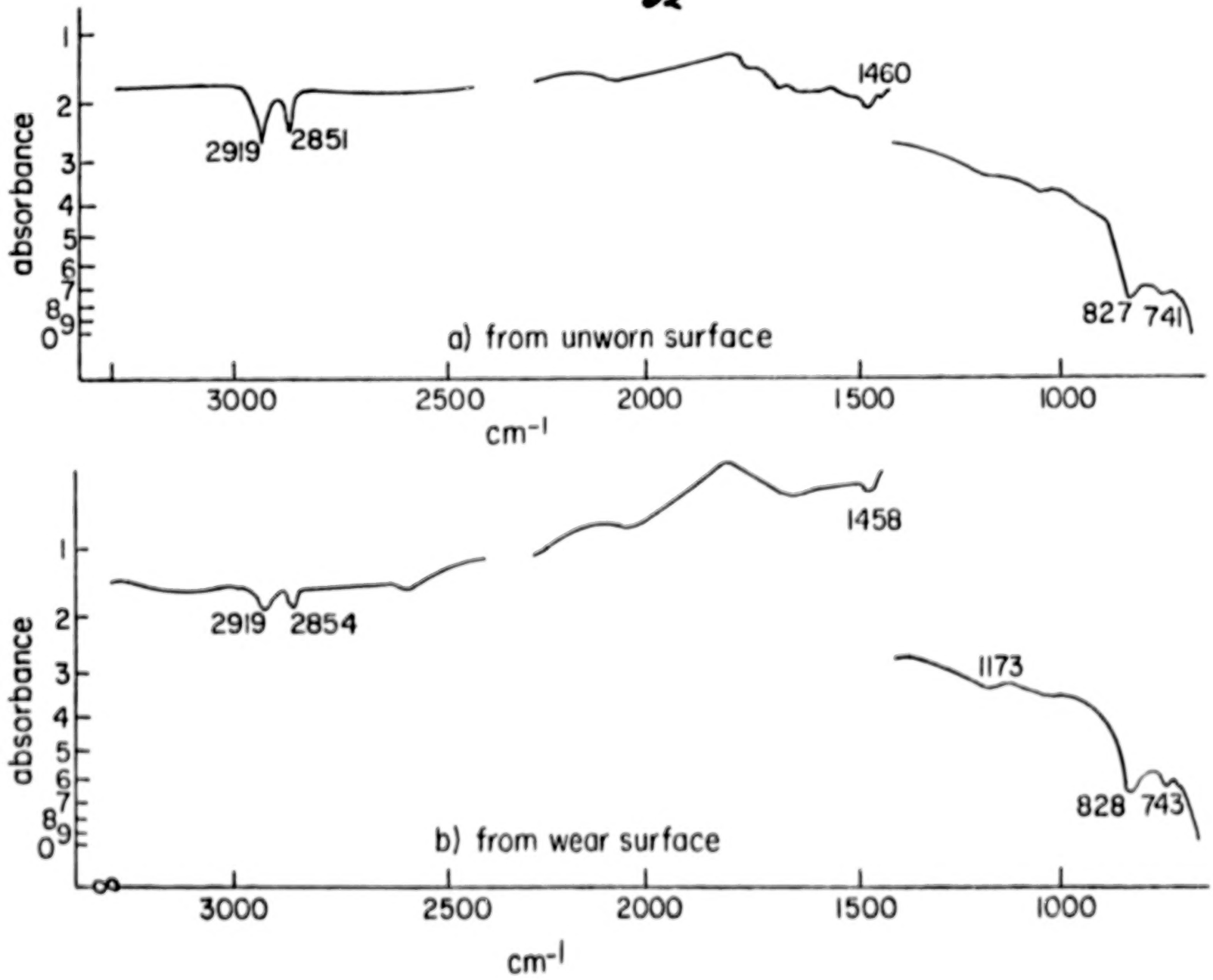

Fig. 17 Reflection spectra of ultrahigh molecular weight polyethylene irradiated with 5 mRad. (a) not worn end, (b) worn part.

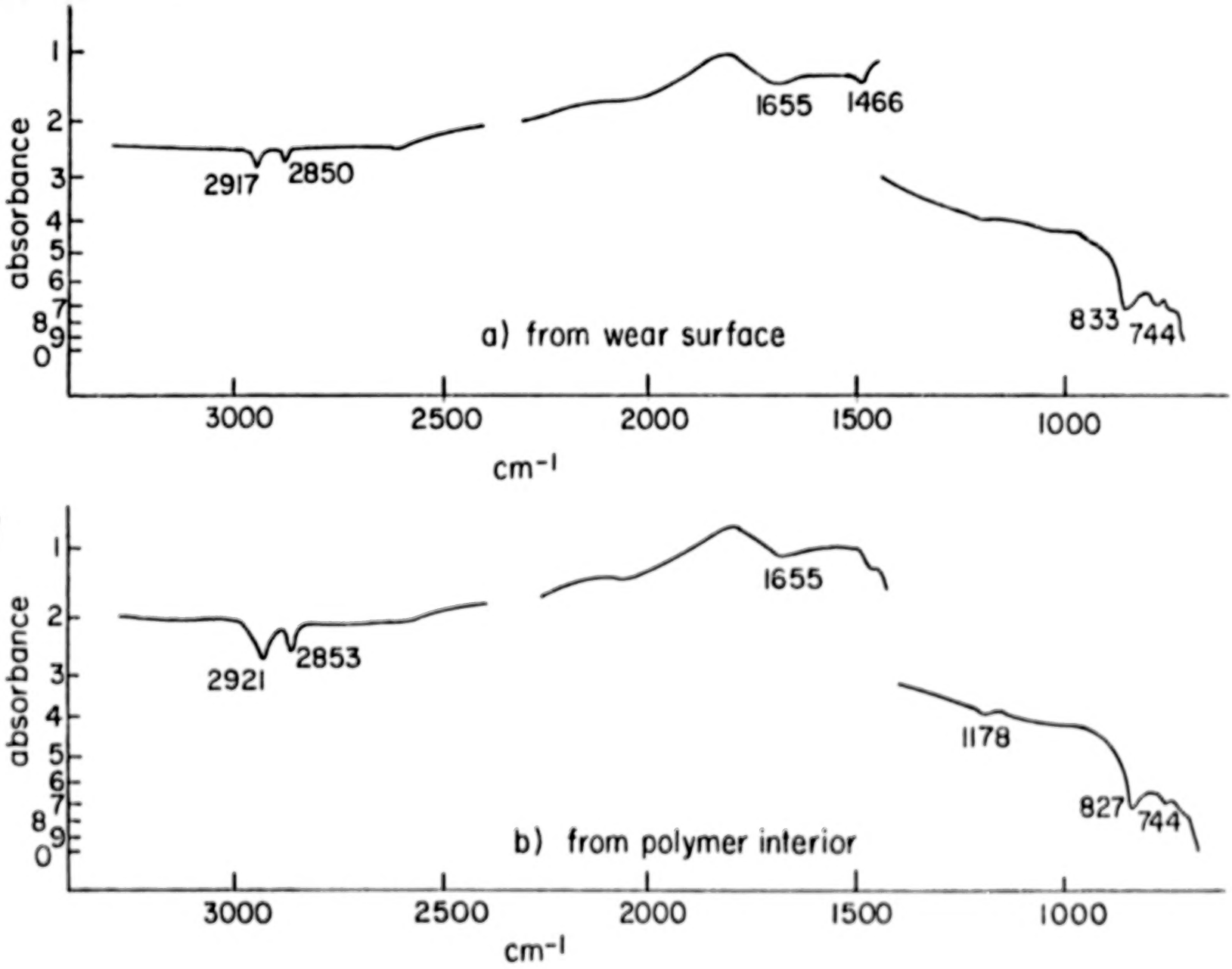

Fig. 18 Reflection spectra of ultrahigh molecular weight polyethylene irradiated with 2.5 mRad. (a) not worn end, (b) worn part.

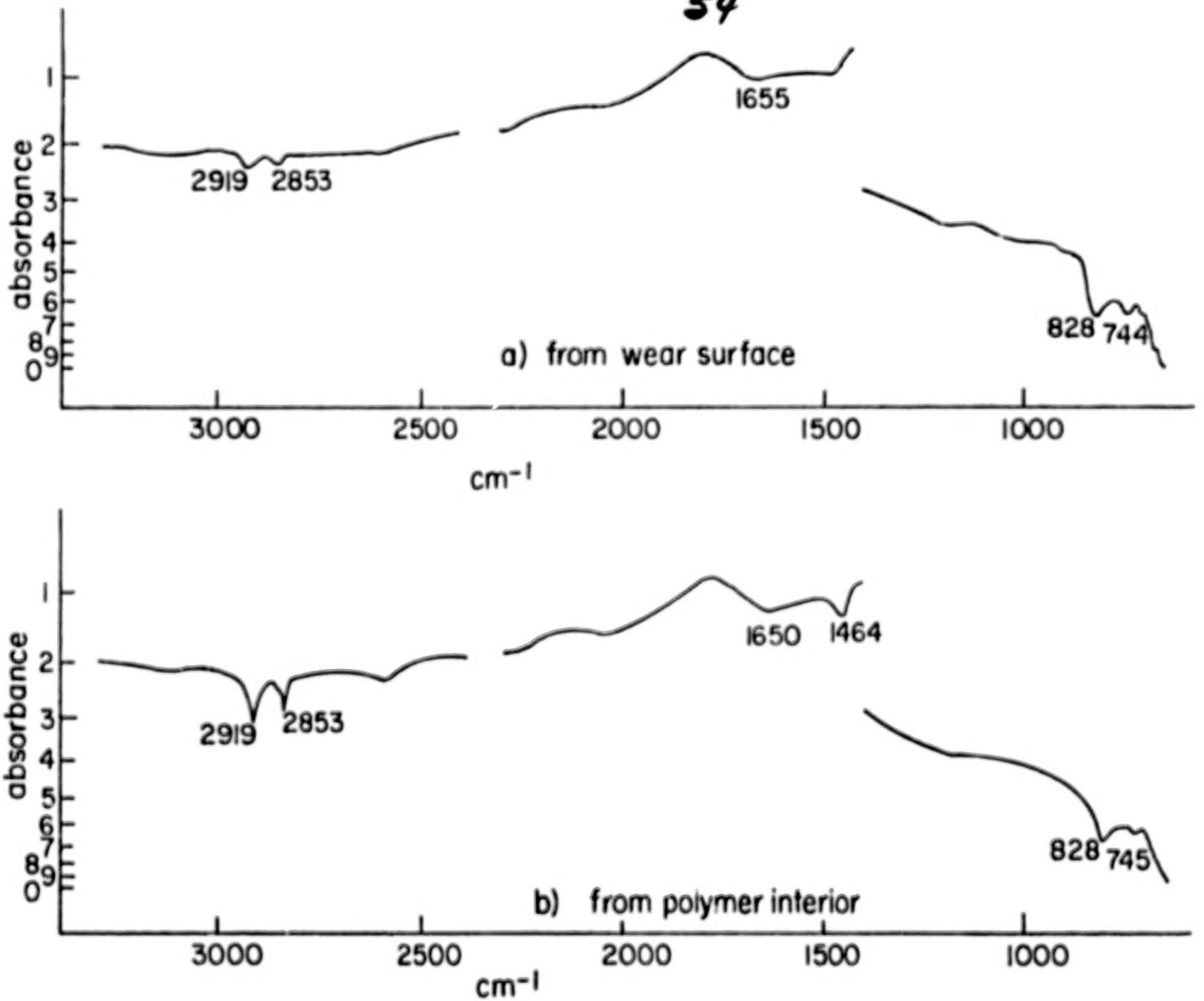

Fig. 19 Reflection spectra of ultrahigh molecular weight polyethylene not irradiated. (a) not worn end, (b) worn part.

1 Report No.	2 Government Accession No.	3 Recipient's Catalog No.
NASA CR-3204		

4 Title and Subtitle	5 Report Date
DETERMINATION OF PHYSICAL AND CHEMICAL STATES OF LUBRICANTS IN CONCENTRATED CONTACTS - PART I	November 1979
	6 Performing Organization Code
7 Author(s)	8 Performing Organization Report No.
James L. Lauer	None
	10 Work Unit No.
9 Performing Organization Name and Address	11 Contract or Grant No.
Rensselaer Polytechnic Institute **Troy, New York 12181**	**NSG-3170**
	13 Type of Report and Period Covered
12 Sponsoring Agency Name and Address	**Contractor Report**
National Aeronautics and Space Administration **Washington, D.C. 20546**	14 Sponsoring Agency Code

15 Supplementary Notes

Final report. Project Manager, William R. Jones, Jr., Fluid System Components Division, NASA Lewis Research Center, Cleveland, Ohio 44135.

16 Abstract

The work under NASA Grant NSG-3170 during 1978 is outlined. A Fourier emission infrared microspectrometer was set up on a vibration-proof optical table and interfaced to a dedicated minicomputer. It was used for the recording of infrared emission spectra from elastohydrodynamic bearing contacts. Its range was extended to cover the entire mid-infrared from 2 to 15 μm. A series of experiments with 5P4E polyphenyl ether showed the existence of a temperature gradient through the lubricant in an ehd contact, which is perpendicular to the flow direction. The experiments also show marked polarization of some of the spectral bands, indicating a molecular alignment. Alignment is less evident at high pressure than at low pressure. To account for this behavior, a model has been suggested along the lines developed for the conformational changes observed in long-chain polymers when subjected to increased pressure--to accomodate closer packing, molecules become kinked and curl up. Experiments with a traction fluid showed periodic changes of flow pattern associated with certain spectral changes. These observations will be studied further. A study by infrared attenuated total reflection spectrophotometry was undertaken to determine whether gamma irradiation would change polyethylene wear specimens. The results were negative.

17 Key Words (Suggested by Author(s))	18 Distribution Statement
Fourier transform spectroscopy **Elastohydrodynamics**	**Unclassified - unlimited** **STAR Category 27**

19 Security Classif. (of this report)	20 Security Classif. (of this page)	21 No. of Pages	22 Price*
Unclassified	**Unclassified**	**56**	**A04**

* For sale by the National Technical Information Service, Springfield, Virginia 22161

NASA-Langley, 1979

90%

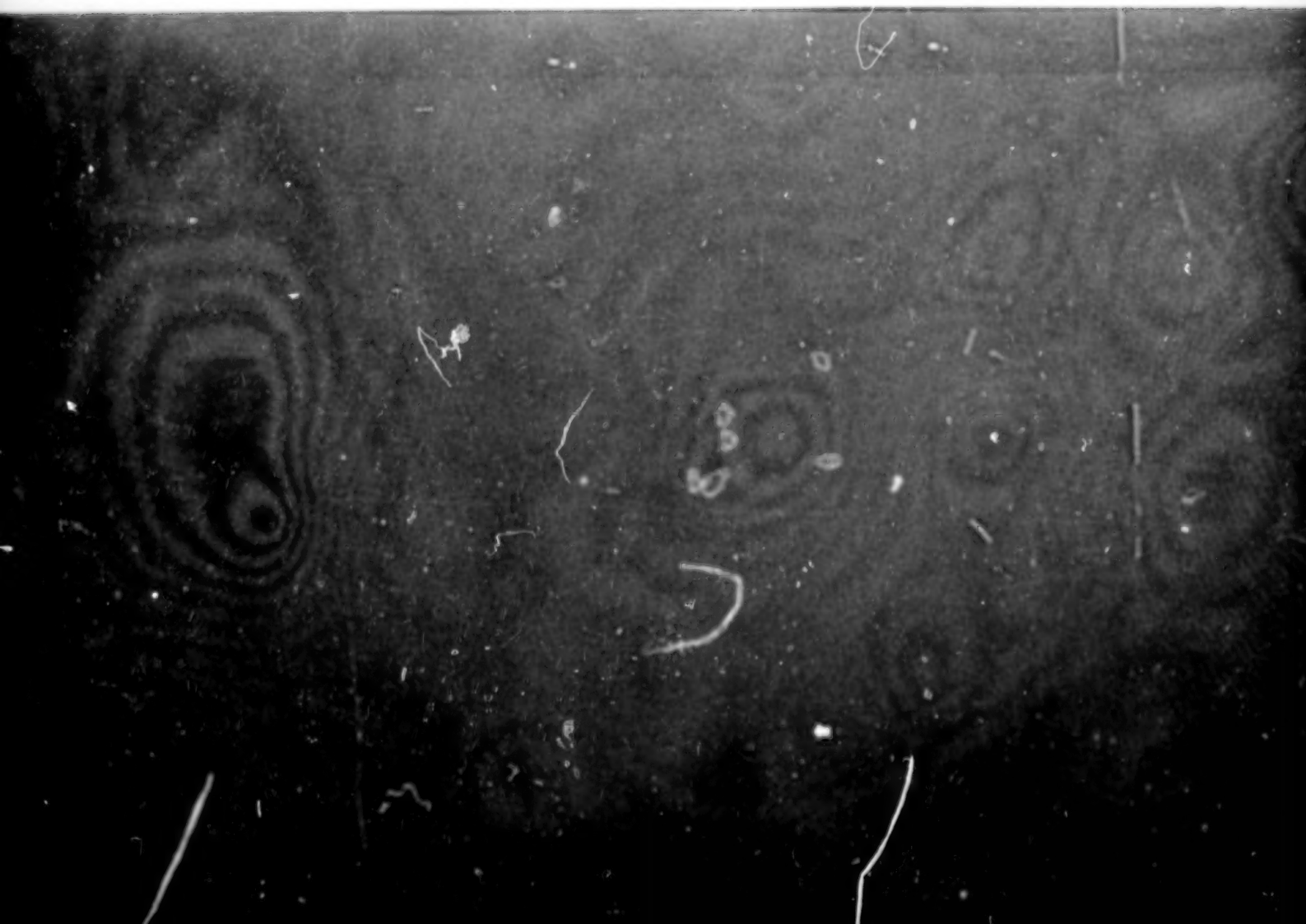

END